NUMERICAL INVESTIGATION OF ENERGY DISSIPATION USING MACRO ROUGHNESS ELEMENTS IN A STILLING BASIN

A THESIS SUBMITTED TO
THE GRADUATE SCHOOL OF NATURAL AND APPLIED SCIENCES
OF
MIDDLE EAST TECHNICAL UNIVERSITY

BY

OĞUZHAN ULUYURT

IN PARTIAL FULFILLMENT OF THE REQUIREMENTS
FOR
THE DEGREE OF MASTER OF SCIENCE
IN
CIVIL ENGINEERING

DECEMBER 2023

Approval of the thesis:

NUMERICAL INVESTIGATION OF ENERGY DISSIPATION USING MACRO ROUGHNESS ELEMENTS IN A STILLING BASIN

submitted by **OĞUZHAN ULUYURT** in partial fulfillment of the requirements for the degree of **Master of Science** i**n Civil Engineering, Middle East Technical University** by,

Prof. Dr. Halil Kalıpçılar
Dean, Graduate School of **Natural and Applied Sciences** _____

Prof. Dr. Erdem Canbay
Head of the Department, **Civil Engineering** _____

Prof. Dr. Mete Köken
Supervisor, **Civil Engineering** _____

Examining Committee Members:

Prof.Dr.A.Burcu Altan Sakarya
Civil Engineering, METU _____

Prof.Dr.Mete Köken
Civil Engineering, METU _____

Prof. Dr. Kerem Taştan
Civil Engineering, Gazi University _____

Assoc.Prof.Dr.Elif Oğuz
Civil Engineering, METU _____

Asst. Prof. Dr. Cüneyt Baykal
Civil Engineering, METU _____

Date: 05.12.2023

I hereby declare that all information in this document has been obtained and presented in accordance with academic rules and ethical conduct. I also declare that, as required by these rules and conduct, I have fully cited and referenced all material and results that are not original to this work.

Name Last name : Oğuzhan Uluyurt

Signature :

ABSTRACT

NUMERICAL INVESTIGATION OF ENERGY DISSIPATION USING MACRO ROUGHNESS ELEMENTS IN A STILLING BASIN

Uluyurt, Oğuzhan
Master of Science, Civil Engineering
Supervisor: Prof.Dr. Mete KÖKEN

December 2023, 77 pages

Stilling basins are often designed using typical types which are suggested by US Bureau of Reclamation (1987). However, in practice there are cases where these typical designs do not dissipate the required amount of energy or produce long hydraulic jumps. In this study, cubic macro roughness elements with different sizes were tested numerically at different chute channel slopes. Relationship between the flow properties and the hydraulic jump length for different macro roughness elements is investigated. Three dimensional numerical simulations using Flow 3D software were run to obtain these relationships. As a result of the studies, the increase in the size of the cubic roughness elements decreased the hydraulic jump length and with cubic roughness elements, shorter hydraulic jump lengths are observed with respect to US Design.

Keywords: Chute Channel, Cubic Macro Roughness Elements, Hydraulic Jump Length, Stilling Basin

ÖZ

ENERJİ KIRICI HAVUZLARDA MAKRO PÜRÜZLÜLÜK ELEMANLARI KULLANILARAK ENERJİ SÖNÜMLENMESİNİN SAYISAL ARAŞTIRILMASI

Uluyurt, Oğuzhan
Yüksek Lisans, İnşaat Mühendisliği
Tez Yöneticisi: Prof.Dr. Mete KÖKEN

Aralık 2023, 77 sayfa

Enerji kırıcı havuzlar çoğunlukla US Bureau of Reclamation (1987) tarafından önerilen tiplerde tasarlanmaktadır. Bununla birlikte pratikte tipik tasarımların istenilen miktarda enerjiyi sönümleyemediği veya uzun hidrolik sıçramaların oluştuğu durumlar da oluşabilmektedir. Bu çalışmada farklı boyutlardaki kübik makro pürüzlülük elemanları farklı dolusavak kanal eğimlerinde test edilmiştir. Farklı makro pürüzlülük elemanları için akım özellikleri ile hidrolik sıçrama uzunlukları arasındaki ilişkiler incelenmiştir. Bu ilişkileri elde etmek için Flow 3D yazılımı kullanılarak üç boyutlu sayısal benzetimler yapılmıştır. Sonuç olarak, çalışma içerisinde belirtilen koşullar altında kübik pürüzlülük elemanlarının ölçüleri arttıkça hidrolik sıçrama uzunluğu azalmaktadır ve kübik pürüzlülük elemanları ile US Design'e göre daha kısa hidrolik sıçrama uzunlukları görülmektedir.

Anahtar Kelimeler: Enerji Kırıcı Havuz, Hidrolik Sıçrama Uzunluğu, Kübik Pürüzlülük Elemanları, Şut Kanalı

To My Family

ACKNOWLEDGMENTS

I profoundly thank my supervisor Prof Dr. Mete Köken for suggesting me working on this fascinating topic. This work would not be possible without guidance and technical support provided by him.

I specially thank my parents, Zahide Hülya Uluyurt and Abdullah Uluyurt for their support of me in finishing this academic study, my sisters Aslı Gülbike Uluyurt and Bilge Tunçel, my friends Serkan Pasinlioğlu, Hüseyin Sebetçi, Mehmet Hakan Bektaş and Sadık Güzel, who supported me in life.

I express my gratitude to every scientist, who sheds light on lives of people. I am happy to be with the people who ask the question why.

TABLE OF CONTENTS

ABSTRACT v

ÖZ vi

ACKNOWLEDGMENTS viii

TABLE OF CONTENTS ix

LIST OF TABLES xi

LIST OF FIGURES xii

LIST OF ABBREVIATIONS xvi

LIST OF SYMBOLS xvii

1 INTRODUCTION 1

1.1 Overview of Stilling Basin, Energy Dissipaters and Roughness Elements 1

1.2 Definition of the Problem 2

1.3 Research Aims & Methodology 4

2 LITERATURE REVIEW 7

3 NUMERICAL INVESTIGATION 11

3.1 Description of the Flow 3D 11

3.2 Description of the Numerical Model 12

3.3 Simulation Setup 23

3.4 Computational Grid 24

3.4.1 Grid Independencies 26

3.4.2 Boundary and Initial Conditions 26

3.4.3 Duration of the Simulations 33

4 RESULTS AND DISCUSSION 35

4.1 Outline of the Numerical Results 35
4.1.1 Results in Chute Channel and Broad Crested Weir 45
4.1.2 Results in the Stilling Basins 50
CONCLUSION 73
REFERENCES 75

LIST OF TABLES

TABLES

Table 3.1 Arbitrary US Dams' characteristic values taken from US Bureau of reclamation website 14
Table 3.2 Physical Quantities of the Model 18
Table 3.3 Simulation done for different broad crested weir height. 34
Table 4.1 The Energy Absorption Percentage in This Study 38
Table 4.2 Average discharges values for 3 different chute channel angles 39
Table 4.3 Hydarulic jump length comparison of 3 meter blocks free surface with fully equipped surface 43
Table 4.4 Flow physical quantities for 0.5 meter broad crested weir 48
Table 4.5 Flow physical quantities for 0.9 meter broad crested weir 50
Table 4.6 The starting point of stilling basin with respect to chute channel angle. 51
Table 4.7 Comparison of Li values from simulations of 60 cm cubic elements and the US Design for different chute channel angles 59
Table 4.8 Distance from the starting point of the jump to end of the chute channel (Li) 60
Table 4.9 The Length of the Hydraulic Jumps 62
Table 4.10 Percentage change in hydraulic jump length with respect to US design for each channel slope 65
Table 4.11 Percentage change and physical difference in hydraulic jump length with respect to US design for each cubic element size 66
Table 4.12 y_2, y_1,and hydraulic jump length values for 20˚ angle chute channel and 0.5 meter height broad crested weir 69
Table 4.13 y_2, y_1, and hydraulic jump length values for 20˚ angle chute channel and 0.9 meter height broad crested weir 71

LIST OF FIGURES

FIGURES

Figure 1.1 Flow Profile at the Stilling Basin 3
Figure 1.2 Chute channel angles that used in this study 4
Figure 1.3 Height of the cubic element (ℓ). 4
Figure 1.4 Coordinate system in the model and origin point 5
Figure 2.1 Hydraulic Jump In Leonarde Da Vinci's Sketches. (De Padova, D., & Mossa, M., 2021) 7
Figure 2.2 Arrangements of roughness elements in Bejestan, M. Shafai & Neisi K.'s study. 9
Figure 3.1 Plans of the Model 12
Figure 3.2 Chute Channel Model for 30 Degree 13
Figure 3.3 USBR Crest Shape (Design of Small Dams, 1987) 15
Figure 3.4 Ogee Crest Shape and Water Profile from 30° Chute Channel 16
Figure 3.5 Flow Profile for the 10 meter long reservoir 17
Figure 3.6 Flow Profile for the 20- meter-long reservoirs 17
Figure 3.7 Flow Profile for 35-meter-long and 70-meter-long Stilling Basins (Stilling basin surface contains 0.4 meter cubic elements) 19
Figure 3.8 From chute channel to stilling basin expected flow profile 20
Figure 3.9 Flow Profile Over Broad Crested Weir 21
Figure 3.10 0.6 m cubic elements along the stilling basin for both fully equipped and non-fully equipped case 22
Figure 3.11 USBR Design Type III stilling basin 22
Figure 3.12 Mesh Sizes in the Reservoir, Over the Ogee Crest and the Chute Channel 25
Figure 3.13 Mesh Blocks, Over the Ogee Crest and the Chute Channel 25
Figure 3.14 Flow Profile for 5 cm and 10 cm Mesh Sizes Stilling Basins 26
Figure 3.15 Chute Channel Mesh Blocks Boundary Conditions 28
Figure 3.16 Stilling Basin Mesh Blocks Boundary Conditions 29

Figure 3.17 Flow on the 10° Chute Channel (Stage 1)..... 30
Figure 3.18 Flow on the Stilling Basin with 0.5 m cubic Roughness Elements (Stage 2)..... 30
Figure 3.19 Top view of the Intersection of Chute Channel and Stilling Basin..... 32
Figure 4.1 Froude Number for 10 Degree Chute Channel..... 36
Figure 4.2 Froude Number for 20 Degree Chute Channel..... 36
Figure 4.3 Froude Number for 30 Degree Chute Channel..... 37
Figure 4.4 Jump Forms specified by Peterka (1958)..... 37
Figure 4.5 Illustrative sketches made by Peterka (1958) for sloping apron. 38
Figure 4.6 Hydraulic jump 2 meter away from the end of the chute channel for broad crested weir height is 1.32 meter..... 39
Figure 4.7 Hydraulic jump 1.8 meter away from the end of the chute channel for broad crested weir height is 1.20 meter..... 40
Figure 4.8 Hydraulic jump 1 meter away from the end of the chute channel broad crested weir height is 0.90 meter..... 40
Figure 4.9 Hydraulic jump for 20˚ chute channel, 0.2 meter cubic elements size and 0.90 meter broad crested weir height..... 41
Figure 4.10 Hydraulic jump for 20˚ chute channel, 0.3 meter cubic elements size and 0.90 meter broad crested weir height..... 41
Figure 4.11 Hydraulic jump for 20˚ chute channel, 0.4 meter cubic elements size and 0.90 meter broad crested weir height..... 41
Figure 4.12 Hydraulic jump for 2 meter cubic elements for broad crested weir height of 1.2 meter with 3 a meter block-free surface. 42
Figure 4.13 Hydraulic jump for 2 meter cubic elements for broad crested weir height of 1.2 meter without blocks-free surface. 43
Figure 4.14 Hydraulic jump when the broad crested weir height is 0.5 meter and the stilling basin has 0.2 meter cubic roughness elements..... 44
Figure 4.15 Hydraulic jump when the broad crested weir height is 0.5 meter and the stilling basin has 0.4 meter cubic roughness elements..... 44

Figure 4.16 Water splashes when the broad crested weir height is 0.5 meter and the stilling basin has 0.5 meter cubic roughness elements 45
Figure 4.17 Broad crested weir for 30° Chute channel. 46
Figure 4.18 Broad crested weir for 20° Chute channel. 47
Figure 4.19 Broad crested weir for 10° chute channel. 47
Figure 4.20 . General view and physical quantities for 20° angle chute channel angle and 0.5 meter height broad crested weir 48
Figure 4.21 General view and physical quantities for 20° angle chute channel and 0.9 meter height broad crested weir 49
Figure 4.22 Flow depth graph for 30 degree chute channel and broad crested weir height of 1.67 meter 52
Figure 4.23 Flow profile at z-x coordinate system for 30-degree chute channel and broad crested weir height of 1.67 meter 53
Figure 4.24 Flow depth graph for 20 degree chute channel and broad crested weir height of 1.58 meter 54
Figure 4.25 Flow profile at z-x coordinate system for 20 degree chute channel and broad crested weir height of 1.58 meter 55
Figure 4.26 Flow depth graph for 10 degree chute channel and broad crested weir height of 1.20 meter 56
Figure 4.27 Flow profile at z-x coordinate system for 10 degree chute channel and broad crested weir height of 1.20 meter 57
Figure 4.28 Distance from the starting point of the hydraulicto end of the chute channel (Li) 57
Figure 4.29 Distance from the starting point of the jump to the end of the chute channel vs cubic elements side length 58
Figure 4.30 Length of jump on the horizontal floor 63
Figure 4.31 Chute Channel Angle-Change in Hydraulic Jump Length with Respect to US Design 67
Figure 4.32 The differences between the lengths and finishing distances of the hydraulic jumps for simulated cases. 68

Figure 4.33 Flow profile for 20˚ chute channel and broad crested weir height is 0.5 meter 70
Figure 4.34 Flow profile for 20˚ chute channel and broad crested weir heihgt is 0.5 meter 72

LIST OF ABBREVIATIONS

ABBREVIATIONS

CFD Computational Fluid Dynamics

DSD Design of Small Dams

EGL Energy Grade Line

HGL Hydraulic Grade Line

METU Middle East Technical University

RNG Renormalized Group

USBR United States Bureau of Reclamation

LIST OF SYMBOLS

Fr_1	Froude number where the hydraulic depth is equal to y_1
h_L	Head lose due to hydraulic jump
y_1	Depth of the water just before the hydraulic jump (m)
y_2	Depth of the water after the hydraulic jump (m)
y_{2s}	Depth of the water just before the broad crested weir (m)
y_c	Critical flow depth (m)
S_0	Slope of the chute channel
L_i	Distance from the starting point of the jump to end of the chute channel (m)
P	Broad crested weir height (m)
P_0	Reservoir depth (m)
H_0	Design head (m)
E	Energy head (m)
B	Channel width (m)

CHAPTER 1

INTRODUCTION

1.1 Overview of Stilling Basin, Energy Dissipaters and Roughness Elements

Stilling Basin is a hydraulic structure where the engineers want to dissipate the excessive energy of water with the formation of hydraulic jump. There are typical basin types which are designed by US Bureau of Reclamation and published in 1987. One of the example to these types of basin is type III basin that is used when the Froude number is larger than 4.5 and velocity is smaller than 15 m/s.

For the design of the Type III, numerous experiments were performed using various types and arrangements of baffle blocks to find better shape by Peterka (1958). The cubic baffle blocks were effective when the best height, width, spacing, and position on the apron were found according to Peterka's studies. Baffle blocks get damaged at high velocities. Therefore, in the simulations fluid physical properties were limited with the Type III design criterias.

Energy dissipaters are structures located on stilling basin to shorten length of hydraulic jump. Energy dissipaters for stilling basins are named according to their positions in the basin. If blocks are located in chute channels, they are named "chute block" or if they are at the end of the basin, they are named "end sill". Energy dissipaters which are located at the middle of the basin, are called baffle blocks. Baffle blocks are used for relatively smaller velocity values because there are concerns with high velocity flows and possible damage to the baffle blocks or the floor of the stilling basin due to cavitation or erosion by sediment-laden flows. (Finnemore, E. J., & Franzini, J. B., 2002)

When these baffle blocks take up too much floor space, they tend to act more like sills than individual blocks. Tests made by Blaisdell (1959) indicate that blocks should occupy between 40 and 55 percent of the stilling basin's floor.

Roughness elements are attached grains to the flume that change the channel roughness. (Tran, C. K. Et al.,2022). The cubic elements placed on the stilling basin in this study as the macro roughness elements on the surface. However, they behave like a baffle block when the block size are greater than flow depth.

1.2 Definition of the Problem

The effect of the blocks in the stilling basin which is situated at the downstream of a chute is investigated within this study. The potential energy stored in the reservoir is converted into kinetic energy at the toe of the chute channel.

The fluid stored in the reservoir passes through the Ogee crest and enters the chute channel, during which the flow regime changes from subcritical flow to supercritical flow. When the chute channel ends and the stilling basin starts, the fluid enters the horizantal slope from the steep slope and this time transitions from the supercritical flow to the subcritical flow occurs. In this transition, hydraulic jump is formed.

Hydraulic Jump formation is changed with the conditions like surface roughness, blocks geometry and length, discharge, slope of the chute channel, starting point of the roughness elemnts, tailwater depth etc. Blocks are used to increase energy dissipation by impact action.

For the hydraulic jump formation at the stilling basin, the expected flow profile is drawn in Figure 1.1.

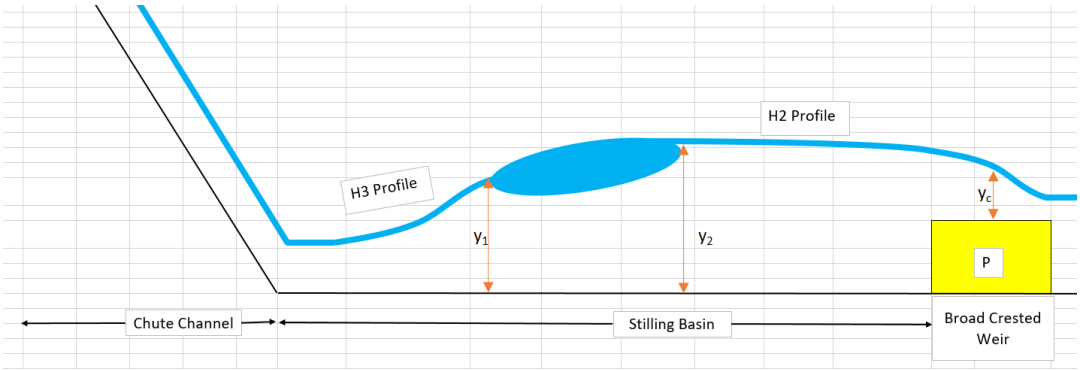

Figure 1.1 Flow Profile at the Stilling Basin

Head loss due to hydraulic jump is directly related with the depth of the incoming flow and Froude Number because as it seen from the Figure 1.1 broad crested weir is located at the end of the basin. Tailwater level is controlled with the broad crested weir (y_2 is constant). Therefore, y_2 value is constant for each case if the broad crested weir heights are same. But on the other hand, lengths of the hydraulic jump for different baffle block dimesions and orientations are not the same. Therefore, comparison can be made with the hydraulic jump length for energy dissipation.

Applying the momentum equation along the flow direction of a simple hydraulic jump occurring in a smooth rectangular channel, the famous Belanger equation is obtained (Chow, 1959):

$$y_2 = \frac{y_1}{2}(-1 + \sqrt{1 + 8 \times Fr_1^2}) \quad (1)$$

For rectangular channel head loss due to Hydraulic Jump is;

$$h_L = \frac{(y_2 - y_1)^3}{4y_1y_2} \quad (2)$$

1.3 Research Aims & Methodology

Energy loss occurs in the shortest length will be the issue that we will consider in our studies in terms of energy loss efficiency. For this reason, energy loss efficiency will be measured by comparing the hydraulic jump lengths in the simulations solved in Flow 3D.

During this study, 3 different channel angles and 5 different cubic element sizes were used. Depending on the angle used, the length of the chute channel changes as the water level at the reservoir is fixed at specific level. Drawings prepared for 3 different angles is shown in Figure 1.2.

.

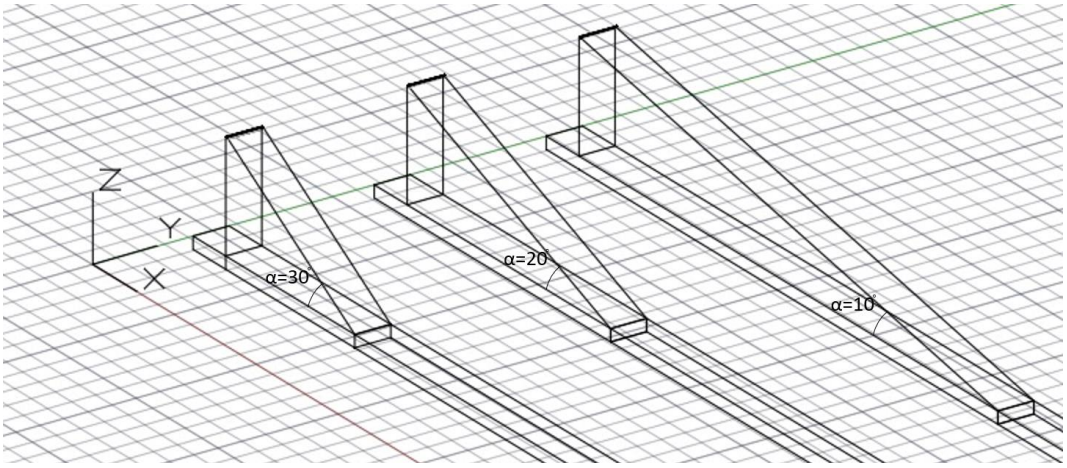

Figure 1.2 Chute channel angles that used in this study

The other changed parameter is length of the cubic elements (ℓ) which is shown in Figure 1.3.

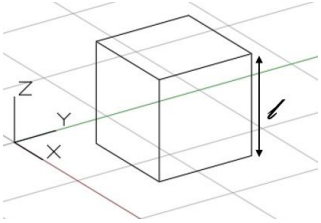

Figure 1.3 Height of the cubic element (ℓ).

In this research the aim is obtaining hydraulic data from simulations to see effects of cubic elements according to their size under the same flow properties. Moreover, to compare the hydraulic data with US Design, type III model were solved as well. At the end of the stilling basin broad crested weir is located to control flow depth at the basin.

In the scope of the study, x-y-z coordinate system is started from the edge of the model. As it can be seen from the figure reservoir base and surface of the stilling basin starts from the z=5 meter. Origin point and x, z coordinate were shown in Figure 1.4.

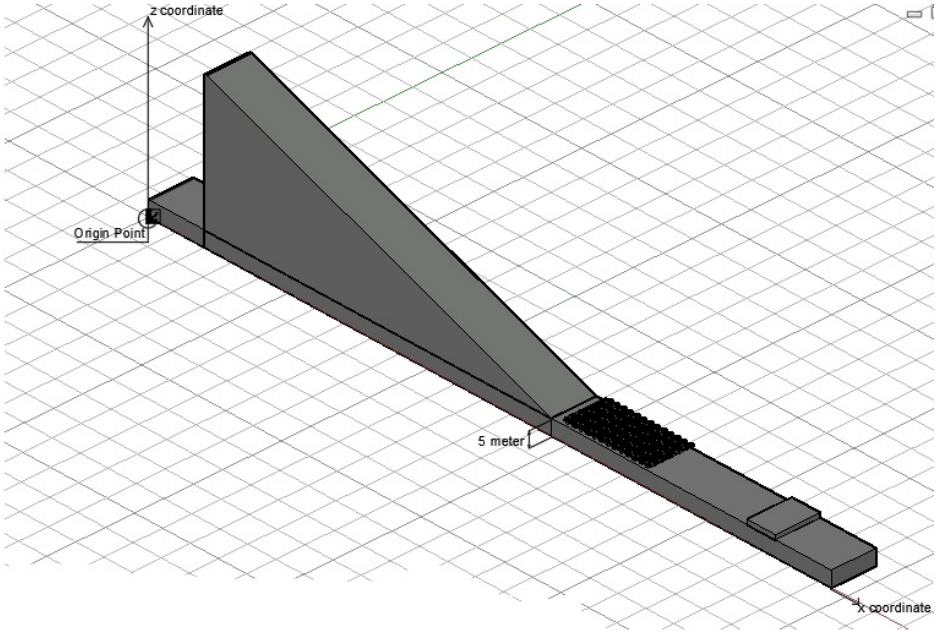

Figure 1.4 Coordinate system in the model and origin point

CHAPTER 2

LITERATURE REVIEW

The roughness elements in the stilling basin had been studied in many studies. In this study main focus is Hydraulic jump phenomena. Its noticed by Leonardo da Vinci and sketched in his works which is shown in Figure 2.1

Figure 2.1 Hydraulic Jump In Leonarde Da Vinci's Sketches. (De Padova, D., & Mossa, M., 2021)

Peterska (1958) studied on different shape of baffle blocks to see effectiveness. For the design of the Type III, Numerous experiments were performed using various types and arrangements of baffle blocks to find the better shape. The cubic baffle blocks was effective when the best height, width, spacing, and position on the apron were found.

Rajaratnam (1968) conducted the first systematic experimental study on Jump in roughned basins. While the roughness height ranged between 0.02 and 0.43 as a basin parameter, the Froude number was kept between 3 and 10 in his experiments as a flow parameter. He reported that the jump length on the rough bed halved the length of a smooth jump with a significant increase in energy consumption.

Leutheusser and Schiller (1975) conducted experiments in a horizontal and roughened rectangular open channel flume to study the development of supercritical channel flow and the performance of hydraulic jumps at the downstream of a sluice gate.

Hughes&Flock (1984) investigated the effects of a rough bed on the properties of hydraulic jump. Hydraulic jump characteristics were measured in a horizontal rectangular channel modified to roughened test beds and measurements were made in the Froude number range of 3-10. This studies observations have shown that boundary roughness reduces both the tailwater depth and the length of a hydraulic jump.

Hager and Bremen (1989) investigated the effect of wall friction on the conjugate depth ratio in classical hydraulic jumps both experimentally and theoretically.

Mohamed Ali (1991) investigated hydraulic jump length in a rough bed. In the experiments cubic elements were used. The length of hydraulic jump is clearly reduced by using cube roughness. The results agree quite well with the results of U.S. Bureau of Reclamation (basin II). In the studies cubic elements were used as roughness elements and they covered an area of 10% of the basin in the experiments.

Hydraulic jump characteristics were investigated experimentally on an artificially roughened bed under different flow conditions by *Alhamid, A.A* (1994). Wooden roughness blocks (1.2x1.2x3.0 cm) were used on horizontal rectangular channel bed, over fixed length with density ranging from 0 to 20%. The 12% roughness density provided the optimal basin length for the flow conditions and roughness arrangement considered in this study.

Negm (2002) collected a very large experimental data set and used to develop a design equation for the optimum stilling basin with cube roughness elements. Roughness elements are gradually distributed. Different roughness intensities, different roughness heights and different roughness lengths are taken into account. The length of the free hydraulic jump over the rough bed is taken as an indicator for

the length of the stilling basin. The roughness parameters that produce the minimum length of the jump and thus the hydraulically minimum stilling basin length are determined and specified.

The hydraulic jumps in the corrugated channel beds were investigated experimentally by *Tokyay, Nuray Denli* (2005). In the experiments, 0.20 and 0.26 (t/s which "t" is corrugation height in mm "s" is wave length in mm) values were used as wave steepness. The range of the Froude number was between 5 and 12. As a result, the length of jump on corrugated beds is about 35% less than that for smooth beds. Also, the energy loss in the hydraulic jump in stilling basin with corrugated beds is significantly greater than in smooth beds.

The basin floor is covered with cubic roughness elements and these cubic elements' sharp side are faced with water flow direction as it shown in Figure 2.2 by *Bejestan, M. Shafai & Neisi K.* (2009). Distance between two cubic elements is equal with diagonal length of the square face. It is stated that new roughened stilling basin are shorter than other type of basins. Hydraulic jump length is reduced about 41%.

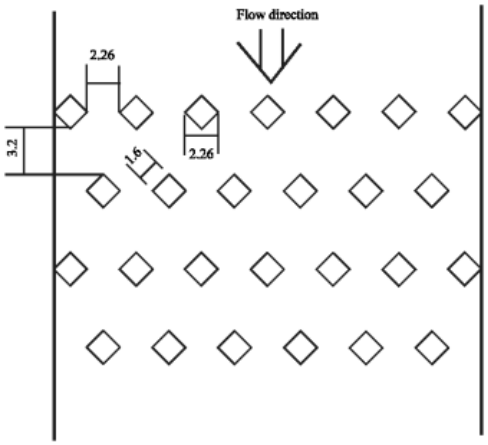

Figure 2.2 Arrangements of roughness elements in Bejestan, M. Shafai & Neisi K.'s study.

Velioğlu, et.al (2015) investigated numerically and experimentally to determine the characteristic of hydraulic jumps on rough beds. Numerical investigations were done by using flow 3D programme. This study proposes that rectangular strip bars as a

roughness elements will stabilize the position of a hydraulic jump and shorten the length of a stilling basin. As results of this study, the tail water depth reduction compared to classical jump is found to be 19% and jump length is reduced by 20%. These roughness elements induce 2% more energy dissipation than that of classical jump.

Pourabdollah, Nahid (2020) investigated, the effects of adverse slope and positive step on hydraulic jump properties including sequent depth ratio, jump length, and energy losses. Four adverse slopes of 0, 0.015, 0.03 and 0.05 (m/m) and two positive step heights of 3 and 6 (cm) was tested. The results showed that although both adverse slope and positive step reduced jump length more than classical jump, the effect of adverse slope was greater than positive step. In the presence of adverse slope and positive step, energy loss was greater than in classical conditions.

The simulations completed in the scope of the study is seperated from other studies with some aspects. Area covered with roughness elements in the stilling basin is 50% of the stilling basin. There is no wall friction factor in the studies as the design created in flow 3d gives opportunities to solve infinetely large channel with symmetrical boundary condition. Stilling basin bed is horizantal , there is no surafece irregularities or positive –negative slope or steps. Different than other studies which includes cubic roughness elements, the designs include reservouir, ogee-crest shape and chute channel parts in the simulations. Therefore, there is possibilities to link design head, body height of the dam and macro roughness elements to each others.

CHAPTER 3

NUMERICAL INVESTIGATION

3.1 Description of the Flow 3D

Computational fluid dynamics programs allow researchers to do numerical investigation. With the development of computer technology, more complex fluid flow simulations can be solved with these programs. To solve the flow over a spillway and stilling basin Flow-3D Software is used in this study. This Software is a user friendly computer program to conduct numerical analyzes. The program is based on finite volume methods. This method divides a geometrically arbitrary domain into a finite number of elements, subsequently used to build finite or control volumes. Flow 3D software basically solve Navier-Stokes equations among these control volumes and gives output of desired physical quantity such as velocity, discharge, pressure etc. at an interested point or region in the domain depending on time. For free surface, the software uses volume of fluid method which is a numerical method of free surface approximation to follow the shape and position of the surface. During the study, FLOW-3D v12.0 Update 1 version of the program were used and processor details of the workstation used in the simulations is Intel® Xeon® Processor E5-2650, 20M Cache, 2.00 GHz, 8.00 GT/s with 16 cores.

3.2 Description of the Numerical Model

The model was prepared in 3 different parts. These are the chute channel & reservoir, the stilling basin & broad crested weir and the roughness elements. These parts' plan are shown in Figure 3.1.

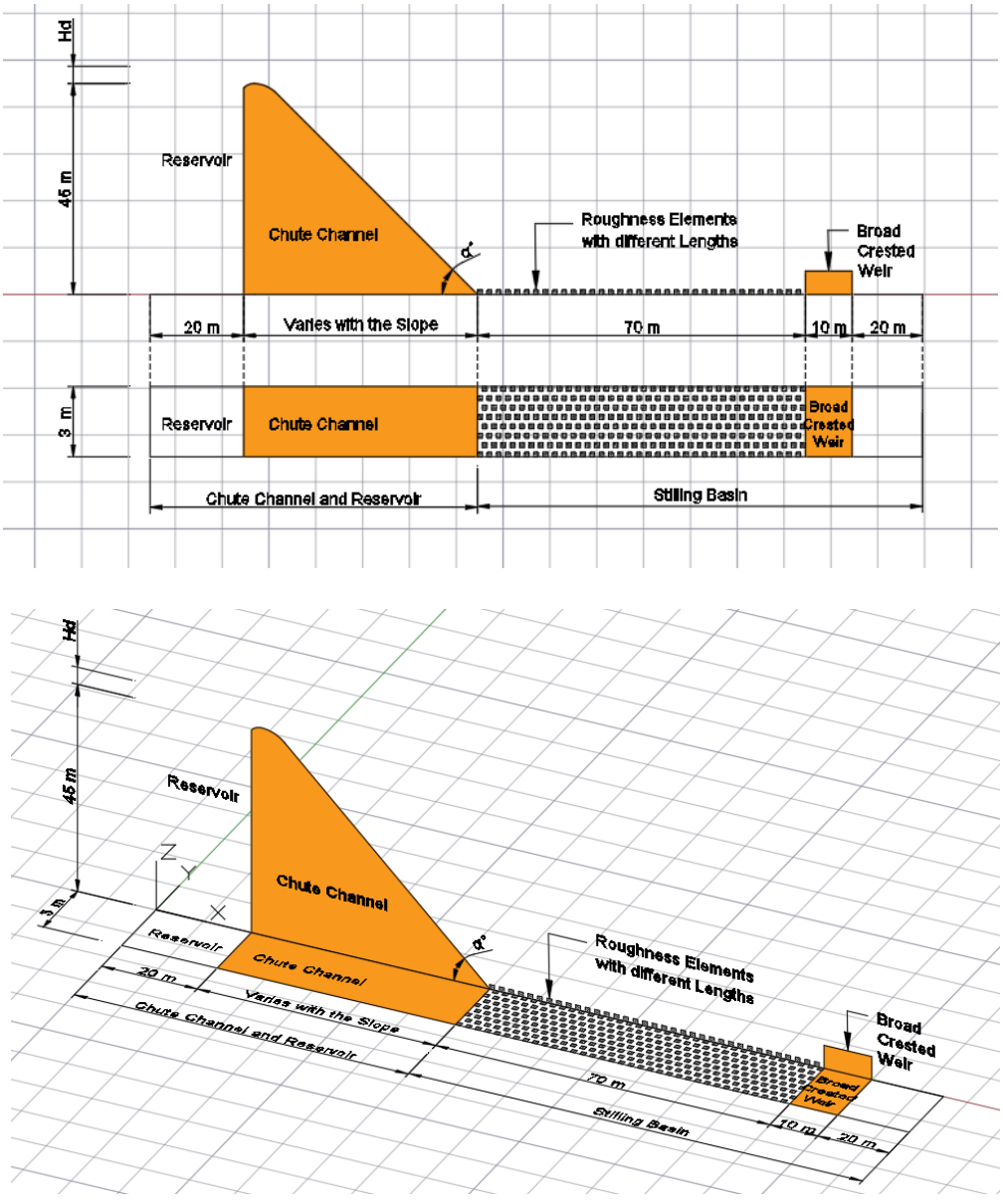

Figure 3.1 Plans of the Model

For the chute channel, the characteristic values of the spillway structures of different US dams have been examined (see Table 3.1). These structures and their data are presented in the Table 3.1. In the light of these data and satisfying the Type III design conditions described in US Bureau of Reclamation, a body height of 45 meters and a design head of 1.5 meters were determined. These values were determined by the designer based on real-life examples.While creating the first part, chute channel design was made in the light of Ogee Crest Shape, slope of the channel and 45-meter body height data. Three different chute angles have been studied, these are 10, 20 and 30 degree angles. The 30-degree model is shown in Figure 3.2.

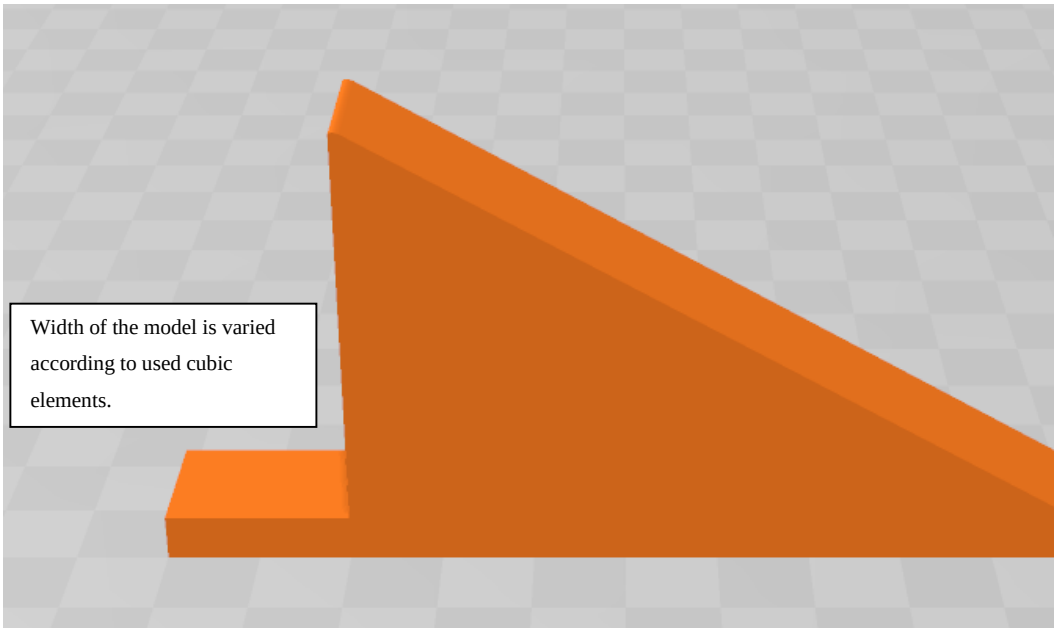

Figure 3.2 Chute Channel Model for 30 Degree

Table 3.1 Arbitrary US Dams' characteristic values taken from US Bureau of reclamation website

	Normal Water Surface Elevation		Hydraulic Height (Normal Operating Depth at Dam)		Base Level		Spillway Crest Elevation		Spillway Operation Water Surface Elevation		Spillway Operating Depth (P+H0)	
	ft	m	ft	m	ft	m	ft	m	ft	m	ft	m
Bonny Dam	3672	1119.23	93	28.35	3579	1090.88	3710.00	1130.81	3736.2	1138.79	157.2	**47.91**
Hoover Dam	1219.6	371.73	576	175.56	643.6	196.17	1205.40	367.41	1232	375.51	588.4	**179.34**
Bully Creek Dam	2516	766.88	92	28.04	2424	738.84	2516.00	766.88	2523	769.01	99	**30.18**
Anita Dam	3003	915.31	30	9.14	2973	906.17	3003.00	915.31	3007.8	916.78	34.8	**10.61**
Big Sandy Dam	6757.5	2059.69	62.8	19.14	6694.7	2040.54	6757.50	2059.69	6762.8	2061.30	68.1	**20.76**
Buckhorn Dam	2803	854.35	72	21.95	2731	832.41	2803.00	854.35	2811.2	856.85	80.2	**24.44**
Bull Lake Dam	5805	1769.36	68	20.73	5737	1748.64	5794.00	1766.01	5805	1769.36	68	**20.73**
Keyhole Dam	4128.7	1258.43	113	34.44	4015.7	1223.99	4099.30	1249.47	4128.7	1258.43	113	**34.44**
Kirwin Dam	1729.25	527.08	97.3	29.66	1631.95	497.42	1757.30	535.63	1773	540.41	141.05	**42.99**

While creating the Ogee crest shape, US Design criteria were taken as a basis. Figure of the ogee crest shape in the US Design and in the simulation are shown in Figure 3.3 and Figure 3.4 respectively. The portion downstream is defined by;

$$\frac{y}{H_d} = -K\left(\frac{x}{H_d}\right)^n \tag{3}$$

Where K and n are constants whose values depend on the upstream inclination which is vertical in our study. The values are 0.5 and 1.87 for K and n, respectively.

On the other hand, the portion upstream from the origin is defined as compound circular curve whose radius values are R_1 = 0.795 and R_2 =0.3525 for vertical upstream inclination according to the design criteria. (Design of Small Dams, 1987)

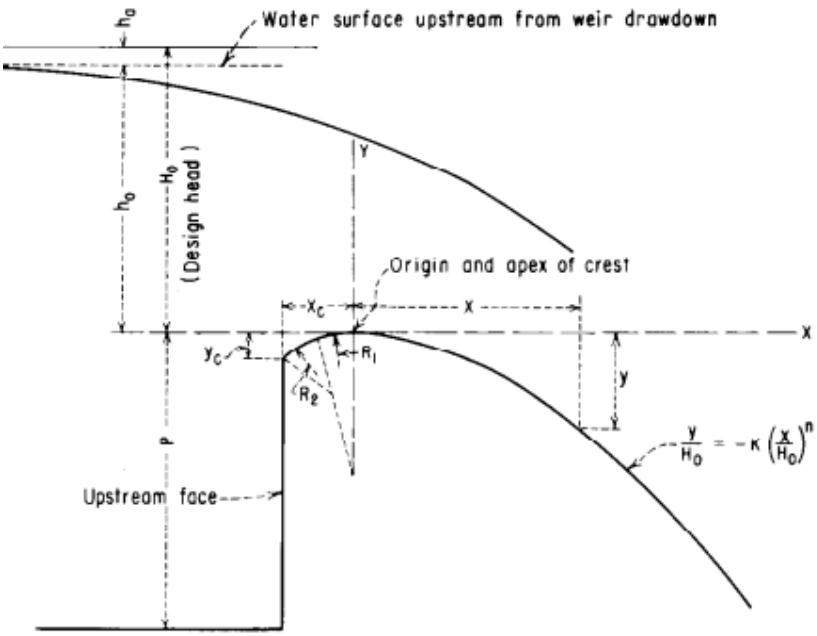

Figure 3.3 USBR Crest Shape (Design of Small Dams, 1987)

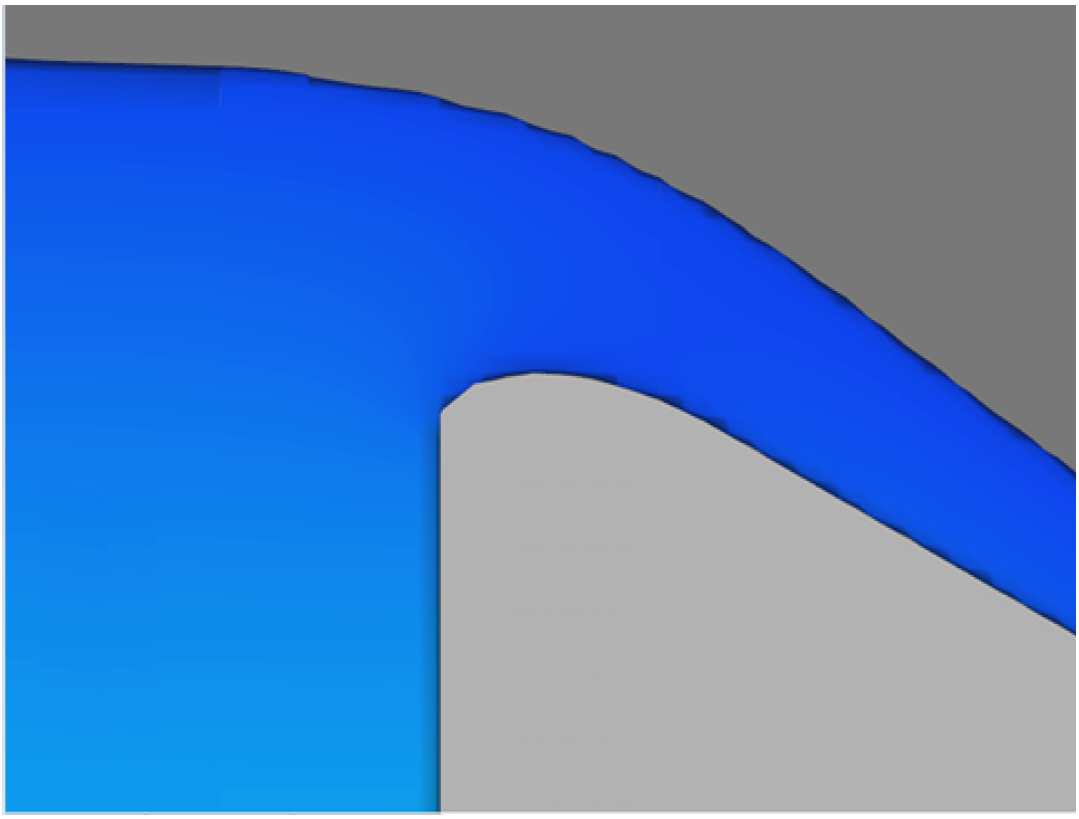

Figure 3.4 Ogee Crest Shape and Water Profile from 30° Chute Channel

The length from ogee-crest to the upstream boundary of the domain is directly related with the amount of water stored in the reservoir. In order to find the reservoir length that will not affect the flow on the chute channel, the flow profile for reservoirs with a length of 10 meters and 20 meters were examined.

Flow profiles obtained from the simulations solved for 10-meter and 20-meter-long reservoirs are presented in Figure 3.5 and Figure 3.6. It is understood from Figure 3.5 that the flow profile on the ogee crest for the 10-meter-long reservoir is affected by this length. Therefore, it was decided to use a 20-meter-long reservoir.

A total of 2790 m^3 of water was stored, with a width of three meters (width change according to satisfying symmetry of macro roughness elements but three meter is arbitrarily chosen for this case) and a height of 46.5 meters, in a 20-meter-long, flow profile seems to have remained unaffected by the length.

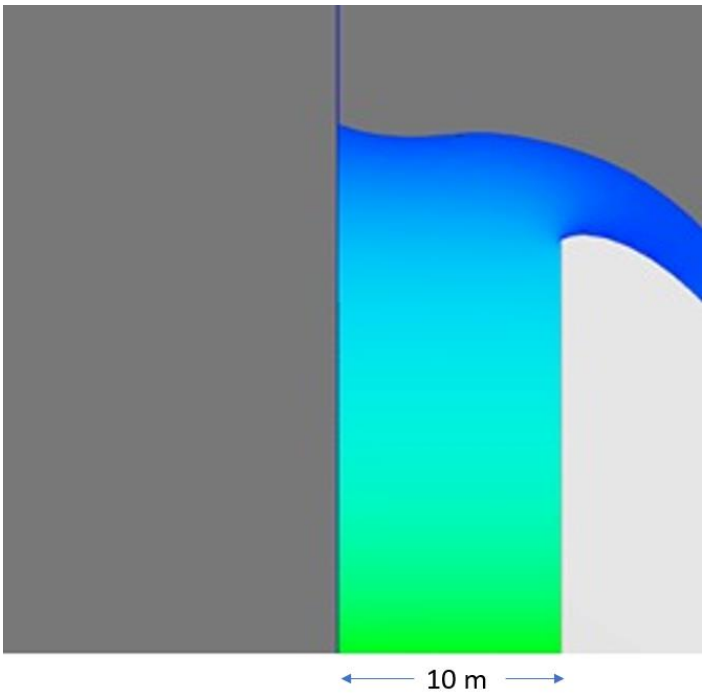

Figure 3.5 Flow Profile for the 10 meter long reservoir

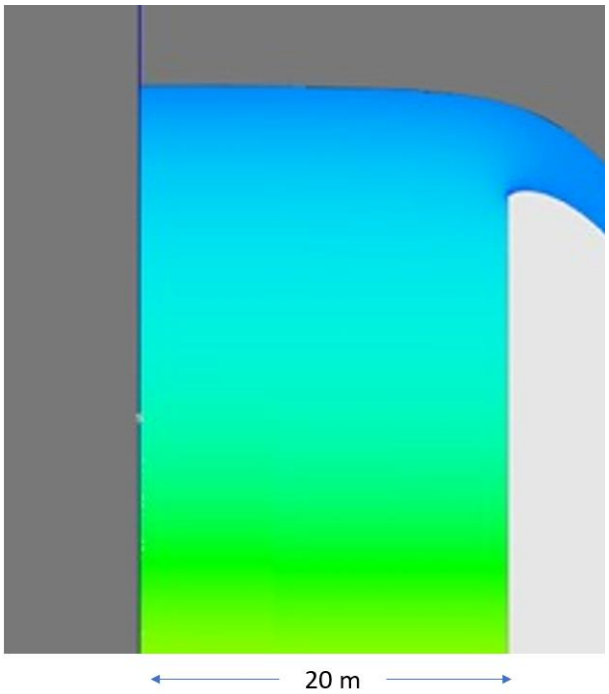

Figure 3.6 Flow Profile for the 20- meter-long reservoirs

The basic physical values determined for the simulation with the obtained data are summarized in Table 3.2.

Table 3.2 Physical Quantities of the Model

			Value	**Unit**
E	(Energy Head)	=	46.5	m
P_0	(Reservoir Depth)	=	45.0	m
H_0	(Design Head)	=	1.5	m
B	(Width)	=	3.0	m
Upstream Slope of the Reservoir		=	Vertical	
Chute Channel Slope (S_0)		=	10-20-30	Degree

Stilling basin consists of three divisions. The first division is a 70-meter-long surface equipped with roughness elements. In the second division, a 10-meter-long broad crested weir was placed and in the third division, there is a smooth surface 20 meters long. (see Figure 3.1)

The first division of the stilling basin is modeled 70 meters long. There are two different design. In one, the entire stilling basin is filled with macro roughness elements.

To measure the adequacy of 70-meter length stilling basin, it was compared to a 35-meter long model's solution and no differences on the free surface profiles were observed. The comparison was done with 0.4 m cubic elements and entire stilling basin is filled with macro roughness elements. Obtained results are given in Figure 3.7.

The simulations were carried out with 70-meter-long stilling basins.

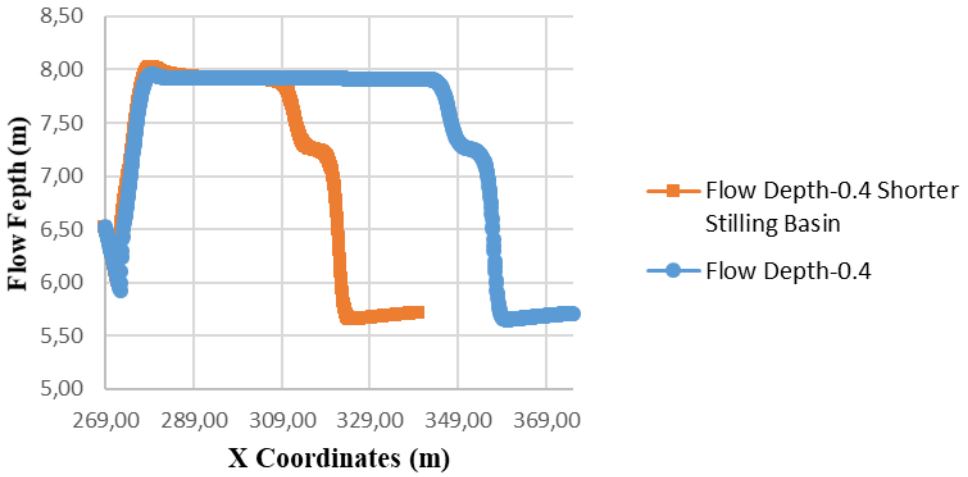

Figure 3.7 Flow Profile for 35-meter-long and 70-meter-long Stilling Basins (Stilling basin surface contains 0.4 meter cubic elements)

To see the effect of stilling basin which is fully equipped with roughness elements over the hydraulic jump the model rearranged and roughness elements started 3 meter away from the end of the chute channel. Roughness elements location were finished away from the broad crested weir not to affect flow depth over it. As the 35-meter length is already enough to see hydraulic jump, roughness elements were located along 35 meters.

The second division, after a 10-meter-long broad-crested weir was placed to control the tailwater depth in a specified level for all roughness elements options. When the flow in the chute channels were solved for 3 different angles, the water depths and unit discharge at the upstream of the hydraulic jump were determined.

To control the tailwater depth on the surface of the stilling basin, broad crested weir is placed.

Physical data such as the unit discharge, flow depth and velocity of the water at a supercritical level through the chute channel were obtained, which is solved with the predetermined Design Head and Energy Head. These data, which will be used in the second stage, also enable us to calculate the depth of the water at the subcritical level

as a result of a hydraulic jump by using the energy equation. Flow depth (y_2) is decided with trial and error method by changing broad crested weir height.

Therefore, Flow depth (y_2) values will vary with broad crested weir height. The tailwater depth was fixed in order to control the effluent and to stabilize the inlet and outlet energy values of the water with broad crested weirs' heights. Expected flow profile along the stilling basin is drawn in Figure 3.8

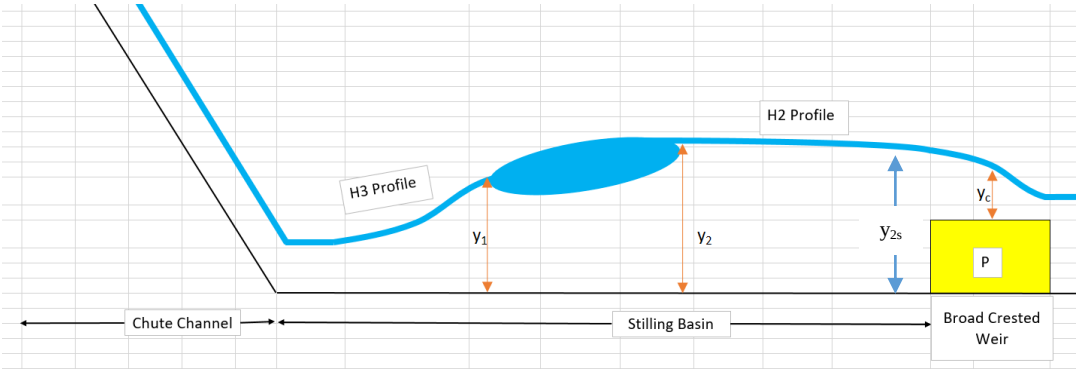

Figure 3.8 From chute channel to stilling basin expected flow profile

Broad crested weir and energy equation used are shown in Figure 3.9 and equation (4).

$$E_{2s} = E_c + P \tag{4}$$

$$y_{2s} + \frac{V_{2s}^2}{2g} = y_c + \frac{V_c^2}{2g} + P \tag{5}$$

$$P = y_{2s} - y_c + \frac{V_{2s}^2}{2g} - \frac{V_c^2}{2g} \tag{6}$$

$$y_c = \sqrt[3]{\frac{q^2}{g}} \tag{7}$$

$$P = y_{2s} - y_c + \frac{q^2}{y_{2s}^2 \times 2g} - \frac{q^2}{y_c^2 \times 2g} \quad (8)$$

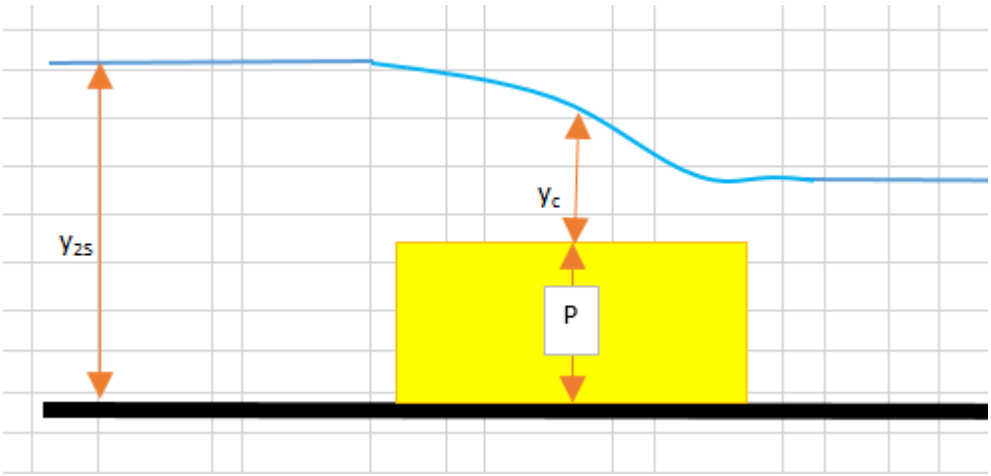

Figure 3.9 Flow Profile Over Broad Crested Weir

The roughness elements are placed on the stilling basin in different sizes. These are 20, 30, 40, 50, 60 cm cubic elements an addition comparison model for Type III stilling basin according to Design of Small Dams is also prepared. The models were created using AutoCAD program in line with the determined characteristics and dimensions. The model having 0.6 m cubic elements both fully equipped, non-fully equipped and the model of USBR Design Type III are shown in Figure 3.10 and Figure 3.11 respectively.

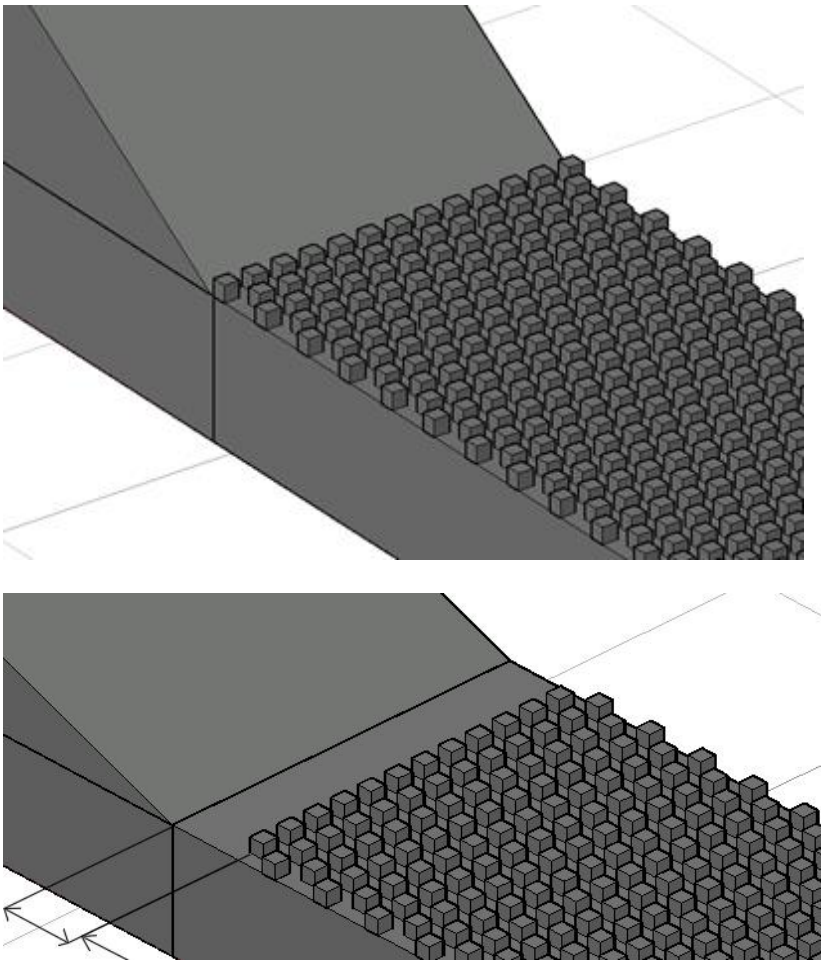

Figure 3.10 0.6 m cubic elements along the stilling basin for both fully equipped and non-fully equipped case

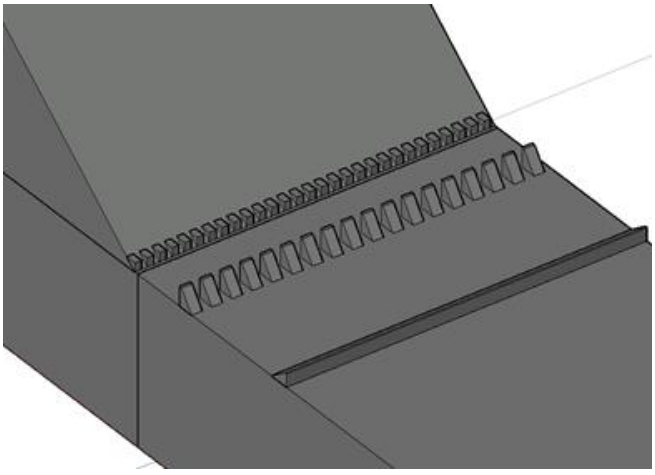

Figure 3.11 USBR Design Type III stilling basin

Simulations were carried out in two stages in order not to repeat the same flow in the chute channel. In the first stage, the flow was just solved in the chute channel. Then, using a continuative boundary condition, this solution is moved to stage two. In the second stage, the simulations were carried out for stilling basin with different roughness elements by using the Restart Simulation feature. Thus, the flow in the chute channel did not have to be repeated.

3.3 Simulation Setup

Flow-3D requires physical rules to be determined initially. Two of the physical models presented by the Flow 3D program were activated and used. These models are “Gravity and Non-inertial Reference” and “Viscosity and Turbulence”. In “Gravity and Non-inertial Reference” tab gravity component activated and the gravity acceleration near Earth’s surface, 9.81 m/s^2, was defined in downward direction.

The Renormalized group (RNG) turbulence model is enabled to include the effects of turbulent flow at the “Viscosity and Turbulence” tab. That model highly recommended by Flow-3D engineers for open channel problems. Viscous flow was chosen, which allows shear forces to develop between the fluid layers. Under the wall shear boundary conditions, no-slip boundary condition was activated which satisfied zero velocity for fluid at a solid boundary. Free surface or sharp interface was activated in interface tracking option and flow mode was set to be “incompressible or limited compressibility”. Fluid properties was specified as 20℃ water.

To describe friction forces in the system, roughness heights were specified for the surface of the models. While roughness height is 0.001 m for the chute channel (ordinary concrete), that is 0.005 m for the stilling basin (course concrete) for the models. (https://www.engineeringtoolbox.com/mannings-roughness-d_799.html)

3.4 Computational Grid

Since the mesh size in the reservoir will not affect the flow over the chute channel, the mesh size was kept as high as possible in the reservoir to avoid time consuming calculations. While in the reservoir mesh size was 40 cm in all three directions, it was decreased to 10 cm step by step at the ogee crest as shown in Figure 3.11. Mesh size was reduced, first from 40 cm to 20 cm, then from 20 cm to 10 cm to avoid interpolation errors and to help overall accuracy of data transferred between the mesh blocks.

Mesh blocks can be added as rectangular prisms in the Flow-3D program. Due to the inclination of the Chute Channel, many mesh blocks have been added along the chute channel to keep the total number of cells low as it shown in Figure 3.12. Therefore, depending on the length of the chute channel, the number of mesh blocks has been increased or decreased. For example, 132 mesh blocks were used in the chute channel with an angle of 10 degrees, while this number is 44 in that of 30 degrees.

Mesh blocks, over the ogee crest and the 30° chute channel is shown in Figure 3.13

For the stilling basin, mesh blocks were used according to the hydraulic jump location. At the jump location block height is kept a little higher with respect to other parts of the stilling basin.

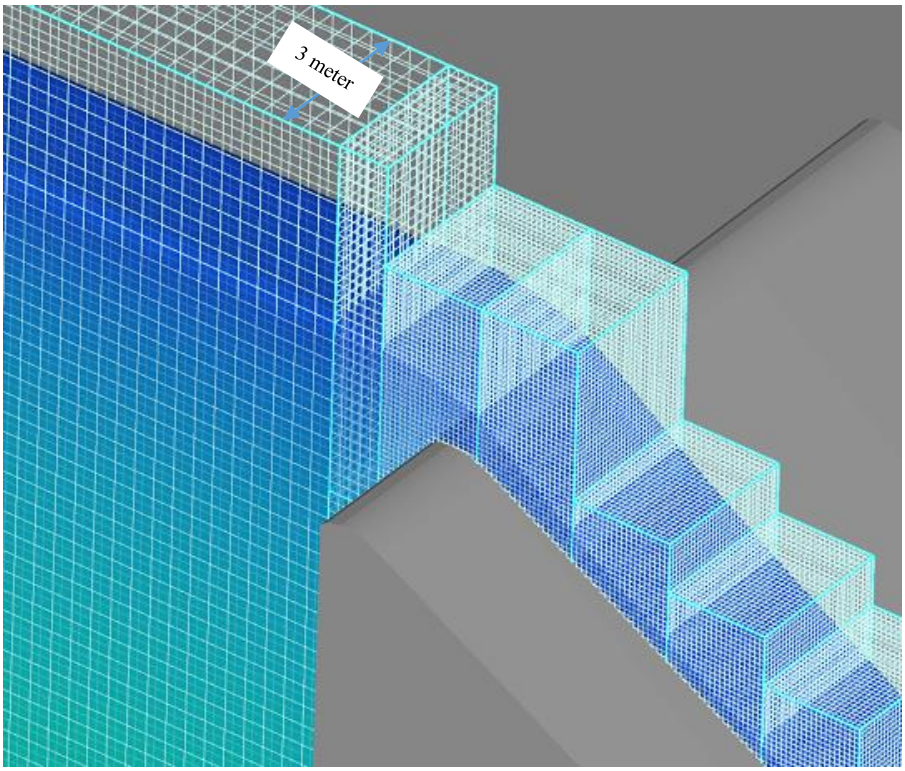

Figure 3.12 Mesh Sizes in the Reservoir, Over the Ogee Crest and the Chute Channel

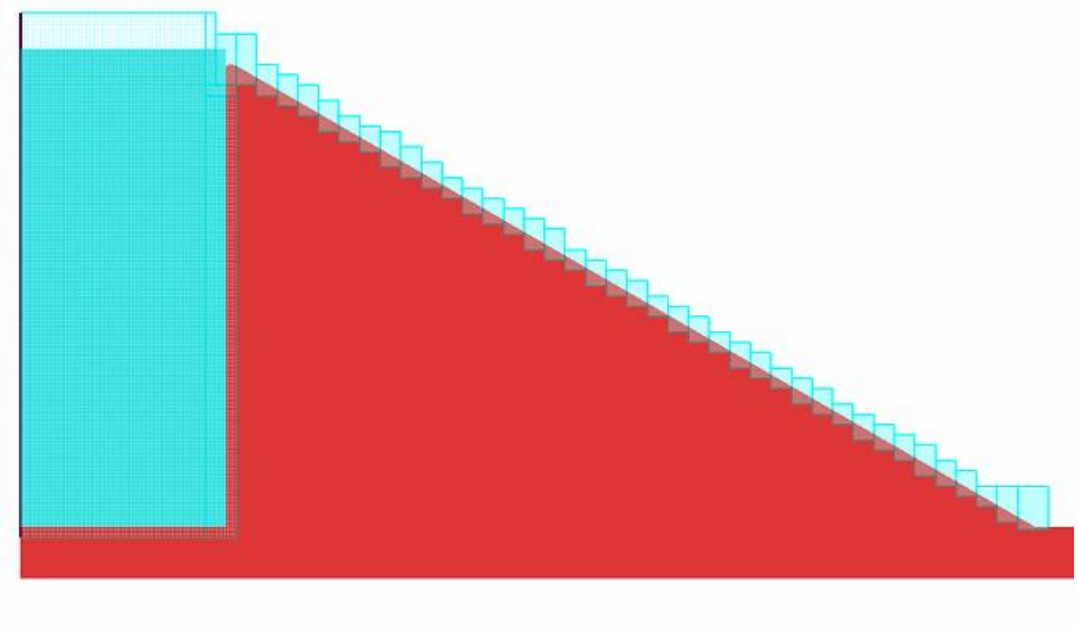

Figure 3.13 Mesh Blocks, Over the Ogee Crest and the Chute Channel

3.4.1 Grid Independencies

Grid size was determined by whether different results were obtained when working with a finer mesh. Grid independencies were checked for chute channel and stilling basin separately.

40 cm-20 cm-10 cm and 20 cm-10 cm-5 cm-2.5 cm mesh size simulations were run to check the grid independencies at the chute channel (part-1). According to the results, the difference in discharge values is under a percent.

10 cm and 5 cm mesh size simulations were run to check the grid independencies at the stilling basin (part 2). As it seen in flow profile shared in Figure 3.14, there is no significant difference in flow depth along the stilling basin. Therefore, 10cm mesh size was used.

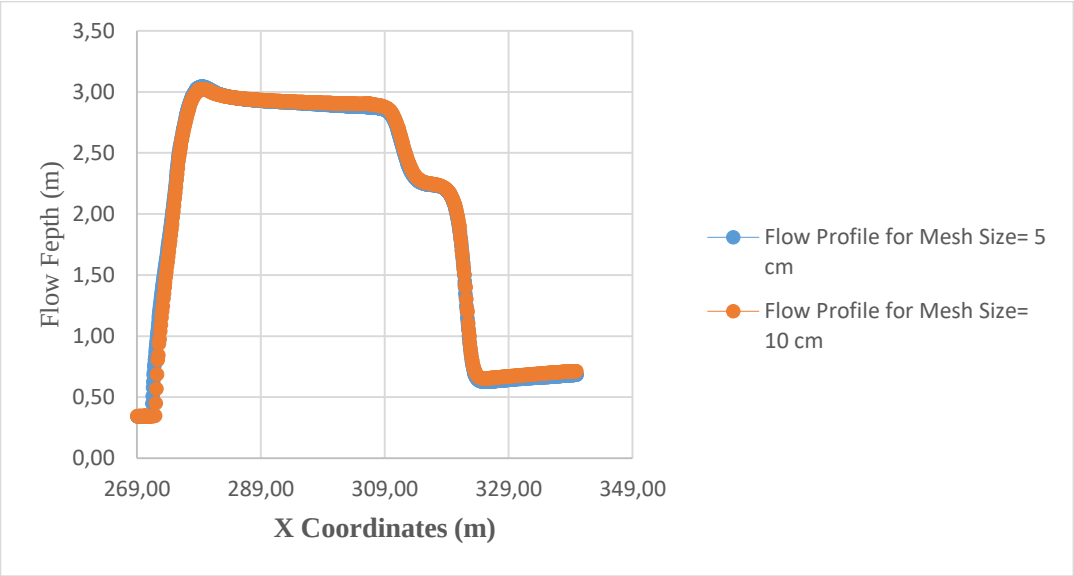

Figure 3.14 Flow Profile for 5 cm and 10 cm Mesh Sizes Stilling Basins

3.4.2 Boundary and Initial Conditions

Flow-3D offers various alternatives for different boundary conditions. Symmetry, pressure, grid overlay and outflow boundary conditions were used in this study.

As stated in the Description of the Numerical Modeling section, the simulations were carried out in 2 stages. In the first stage, the Chute channel was solved. Initially, a water body of 46.5 meters high in the reservoir was defined in order to reach the desired conditions more quickly to stabilize the water level in this reservoir, the water level was kept at a height of 46.5 meters using the pressure boundary condition. Moreover, inlet flow is controlled by 'Specifying fluid elevation' option. Hydrostatic pressure tab is selected for the fluid. As the stagnation condition is the best and most realistic physical condition to use as stated in 'Flow-3D Excellence in flow modeling software User Manual Version 9.3, stagnation pressure checked under the pressure tab in the program. That means, fluid elevation is set as total upstream hydraulic head.

There is no need for downstream control as the flow stream will leave the domain so that 'outflow' boundary condition is given in the last mesh block in the chute channel. Symmetry boundary condition is used on the two lateral sides, whereas no-slip condition is used over the spillway surface as shown in Figure 3.15.

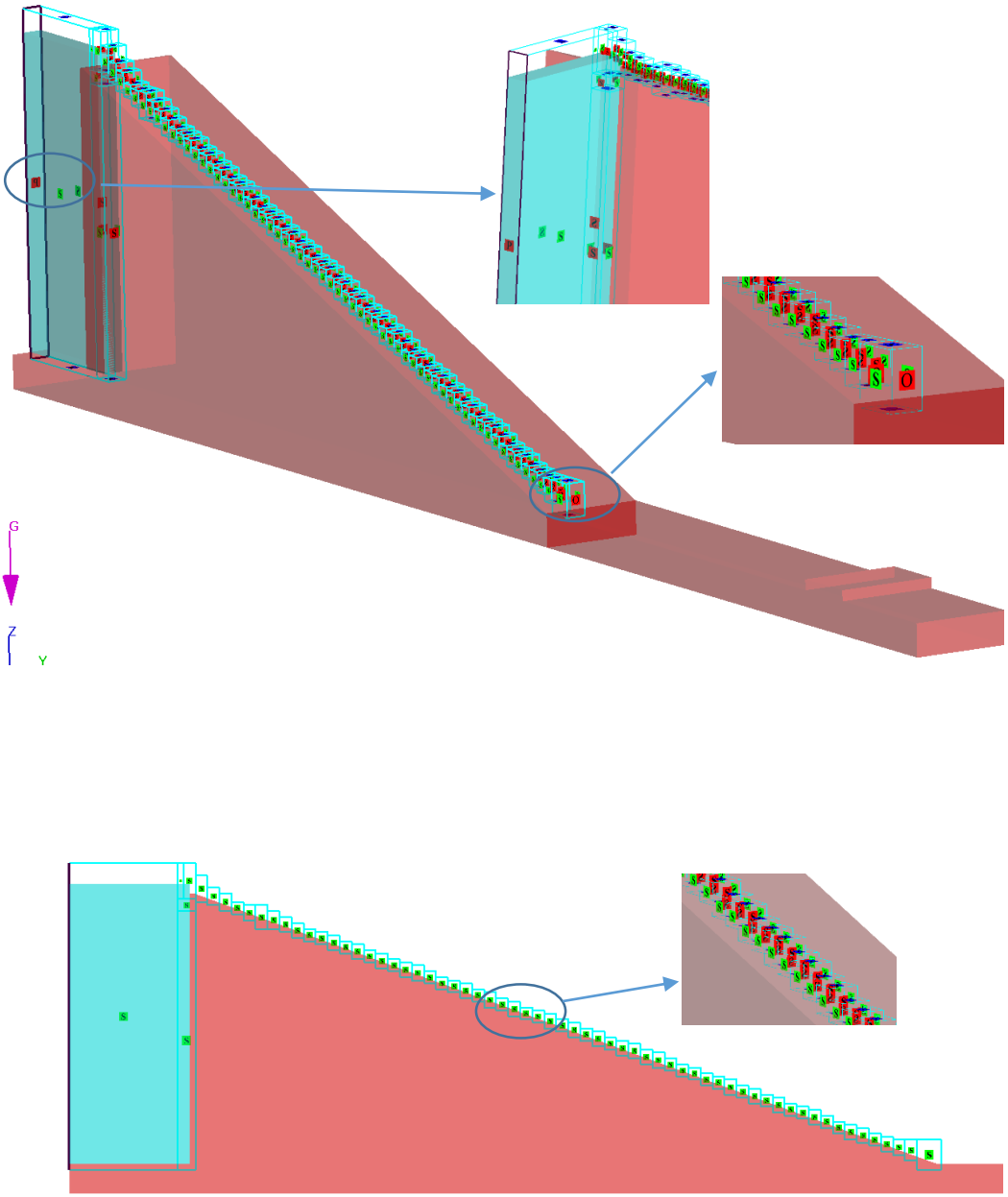

Figure 3.15 Chute Channel Mesh Blocks Boundary Conditions

At stage two, to use data which is obtained in stage one. First mesh block's X_{min} boundary condition was specified as 'Grid Overlay' as shown in Figure 3.16 because flow conditions in the regions are initialized using the data from the restart input file.

For a boundary of the Grid Overlay type, the restart data from the original grid will be used to set all flow parameters at that boundary, which will then be treated as constants throughout the calculation. Unlike the symmetry boundary condition, the grid overlay boundary condition allows to obtain the physical properties of the flow from stage 1.

Likewise, at the stage 1, there is no need for downstream control as the flow stream will leave the domain, so that ‘outflow’ boundary condition is given in the last mesh block for the stilling basin.

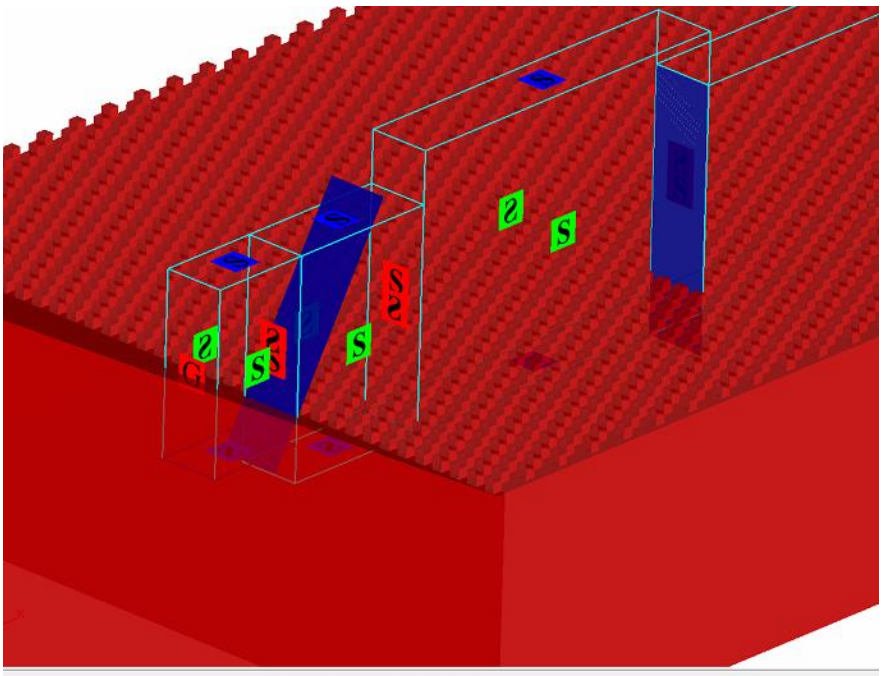

Figure 3.16 Stilling Basin Mesh Blocks Boundary Conditions

The general view of the flow under these boundary conditions in the chute channel and the stilling basin are shared in Figure 3.17 and Figure 3.18. Channel width is 3 meters for stage 1.

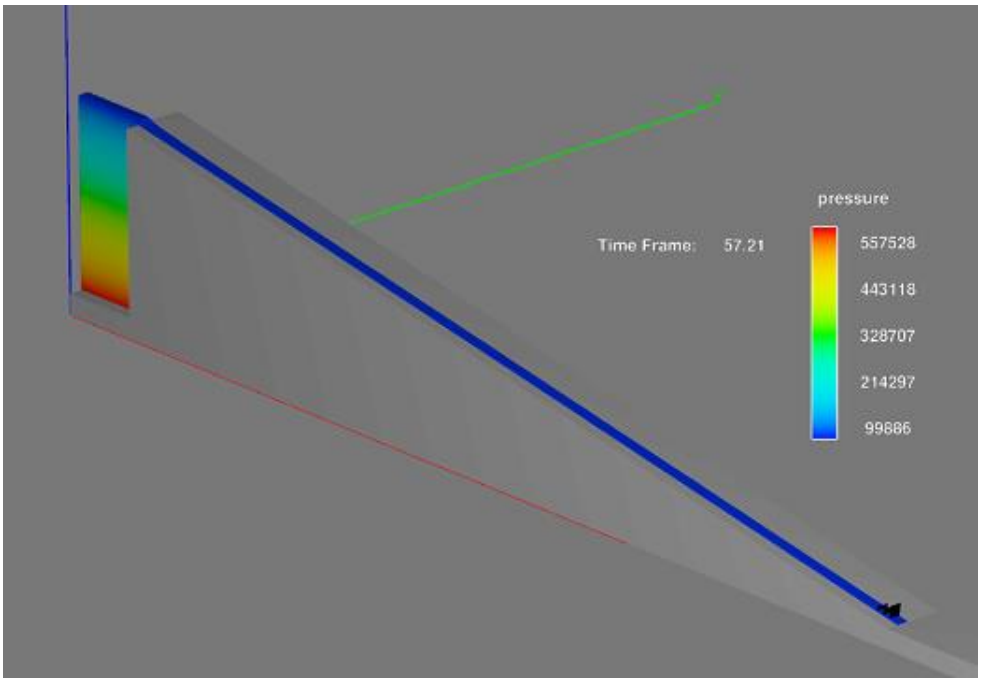

Figure 3.17 Flow on the 10˚Chute Channel (Stage 1)

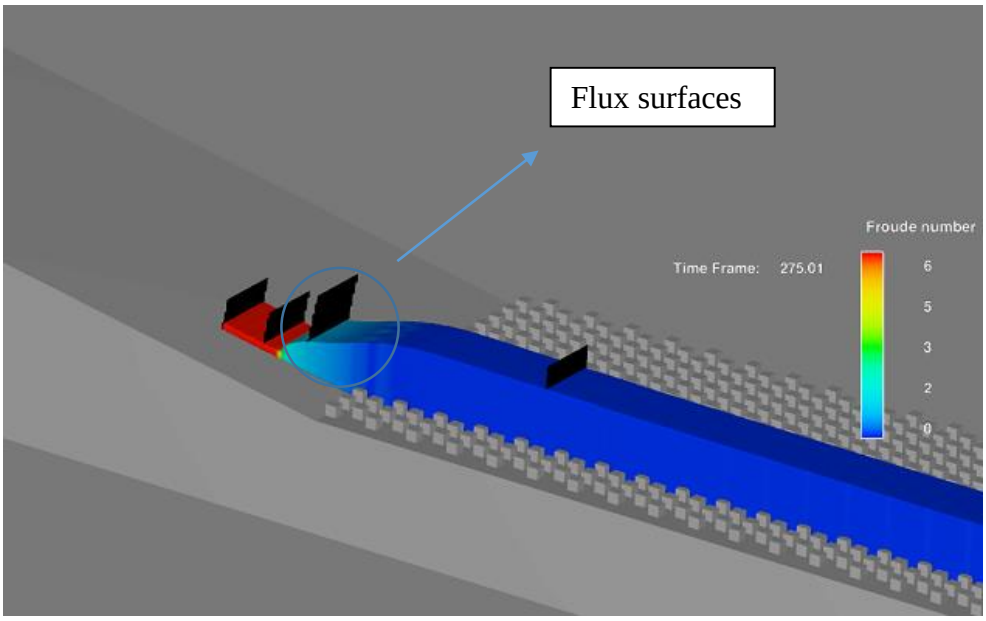

Figure 3.18 Flow on the Stilling Basin with 0.5 m cubic Roughness Elements (Stage 2)

Flux surfaces are not part of the model, in Flow3D program to obtain certain flow properties these imaginary surfaces were added.

In the second stage, the width is reduced in order to provide symmetry according to the dimensions of the cubic elements.

While the width is 3 meters for 50 cm cubic elements, this value is 2.4 meters for 40 cm cubic elements. Likewise, a width of 1.8 meters was used for 30 cm cubic elements and a width of 1.2 meters was used for 20 cm cubic elements. In this way, symmetry condition is satisfied along the lateral boundaries for all the cases. (See Fig.3.19)

Since the flow in the chute channel was simulated for a width of 3 m. In the stilling basin simulation of 60 cm cubic elements a width of 3.6 m could not be used. This is why in satisfying the symmetry condition less number of blocks were used compared to the other cases.

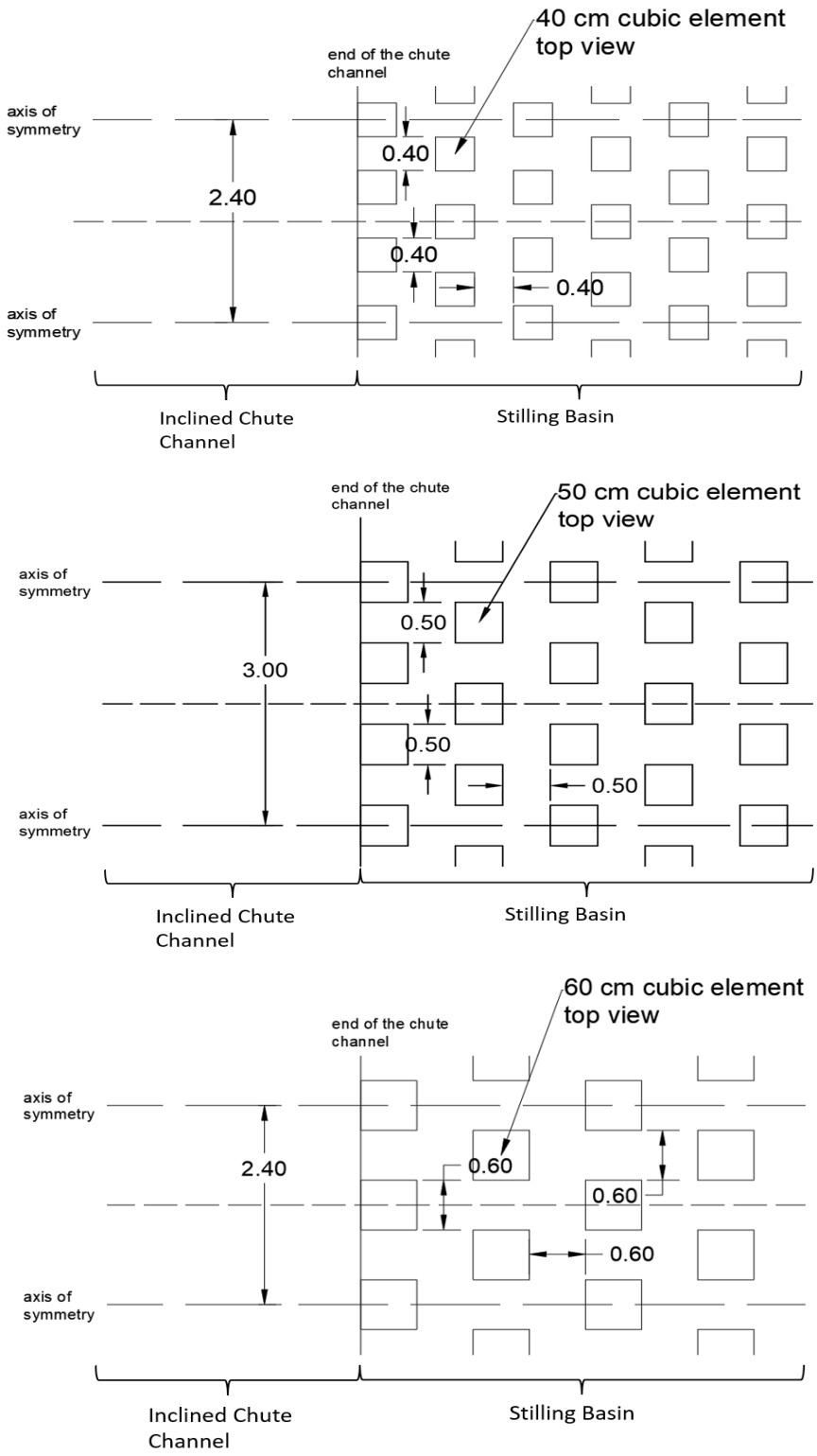

Figure 3.19 Top view of the Intersection of Chute Channel and Stilling Basin

3.4.3 Duration of the Simulations

The simulations continued until the flow reached the steady state. While this process was longer in the chute channel with an inclined angle, it took a shorter time for the relatively less inclined chute channel. Therefore, there is no specified time limit. The same applies to solutions in the stilling basin.

On average, the simulations in the chute channel vary between 1 and 2 days, while each simulation in the stilling basin takes an average of 1 day. The total runtime of all the simulations was approximately 3 months.

Simulations completed for different variables which are S_o (slope of the chute channel), broad crested weir height, roughness element size and distance from the starting point of stilling basin to starting point of roughness elements are shown in Table 3.3.

Table 3.3 Simulation done for different broad crested weir height.

		So (Slope of the chute channel) (degrees)	Broad crested weir height (m)	Roughness elements sizes (m)	Distance from the starting point of stilling basin to starting point of roughness elements (m)
Effect of Channel Angle	Effect of roughness element size	30	1.67	0.6	0
		30	1.67	0.5	0
		30	1.67	0.4	0
		30	1.67	0.3	0
		30	1.67	0.2	0
		30	1.67	US Design	0
	Effect of roughness element size	20	1.58	0.6	0
		20	1.58	0.5	0
		20	1.58	0.4	0
		20	1.58	0.3	0
		20	1.58	0.2	0
		20	1.58	US Design	0
	Effect of roughness element size	10	1.2	0.6	0
		10	1.2	0.5	0
		10	1.2	0.4	0
		10	1.2	0.3	0
		10	1.2	0.2	0
		10	1.2	US Design	0
Effect of tailwater depth		20	1.32	0.6	0
		20	1.2	0.6	0
----------		20	0.9	0.6	0
Effect of tailwater depth and starting point of roughness elements	Effect of roughness element size				
		20	0.9	0.4	0
		20	0.9	0.3	0
		20	0.9	0.2	0
	Effect of roughness element size	20	0.5	0.2	3
		20	0.5	0.3	3
		20	0.5	0.4	3
		20	0.5	0.5	3
Effect of starting point of roughness elements		20	1.2	0.2	3
		20	1.2	0.2	0

CHAPTER 4

RESULTS AND DISCUSSION

4.1 Outline of the Numerical Results

Totally 36 simulations are solved. Three of them were solved in the chute channel for three different slopes.

30 different simulations were solved for different variables at the stilling basin and the results were shared within the scope of the study.

One simulation is solved for a shorter stilling basin to show that the length of the stilling basin is sufficient. Two other simulations are solved to show grid independencies of the study.

The discharge values and Froude numbers in the chute channels were determined for three different angles by solving the simulations. The Froude numbers in the studies were 6.05, 7.60 and 7.75 for different chute channel angles as shown in Figure 4.1, Figure 4.2, Figure 4.3.

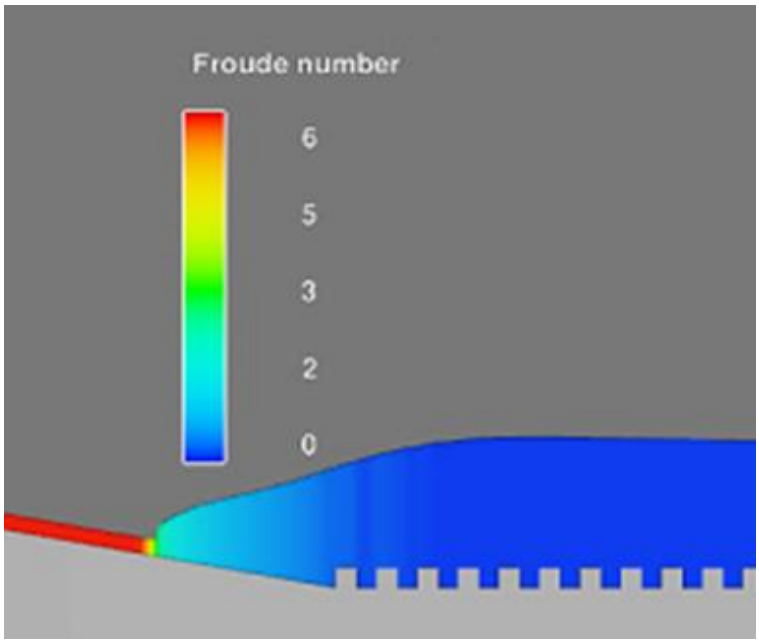

Figure 4.1 Froude Number for 10 Degree Chute Channel

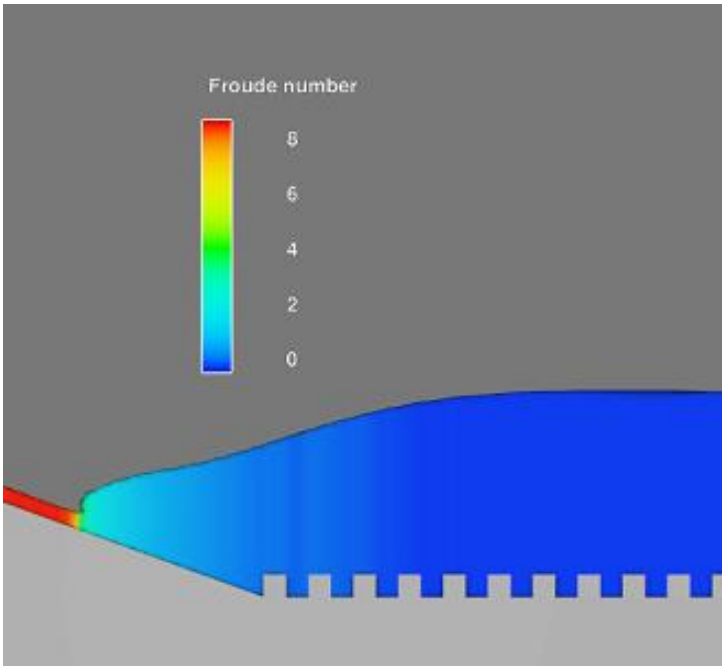

Figure 4.2 Froude Number for 20 Degree Chute Channel

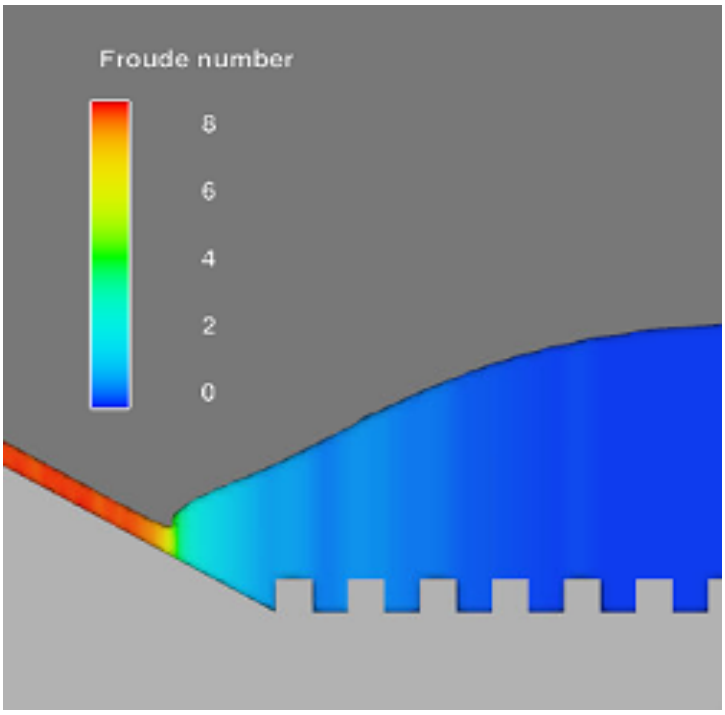

Figure 4.3 Froude Number for 30 Degree Chute Channel

These values shows that Good Jumps were expected for the cases hydraulic jump started at the chute channel according to Jump classification which is shared in Figure 4.4. Peterka (1958) specified that a well-stabilized jump can be expected for the range of Froude numbers from 4.5 to 9. The Jump is well-balanced. Moreover, Peterka (1958) specified the energy absorption in jumping at this range of Froude numbers as from 45 to 70 percent, that values are suitable with the performed studies as it shown in Table 4.1.

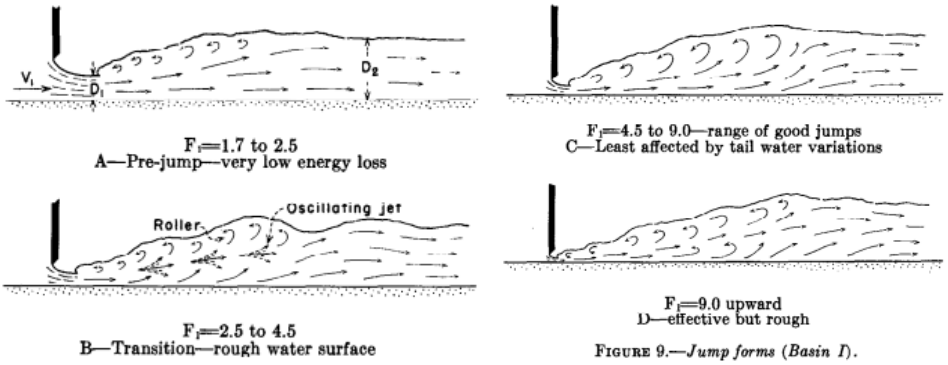

Figure 4.4 Jump Forms specified by Peterka (1958)

Table 4.1 The Energy Absorption Percentage in This Study

		Energy Head Before The Jump		Energy Head After The Jump		Change in Percantage
10 Degree	US Design	6.48	m	3.04	m	46.89%
	0.6 cm cubic elements	6.44	m	3.21	m	49.88%

As can be seen from the rendered images taken from the simulation which are shared in Figure 4.1, Figure 4.2 and Figure 4.3, the hydraulic jump starts over the chute channel for some cases. While designing, the stilling basin elevation and the reservoir base elevation were kept at the same level. The change of this level affects the start of the hydraulic jump. Peterka (1958) defined the hydraulic jump which occurred in the sloped surface as a "stilling basin with sloping apron" design type. The illustrative sketch of the jump is drawn by Peterka (1958) shown in Figure 4.5.

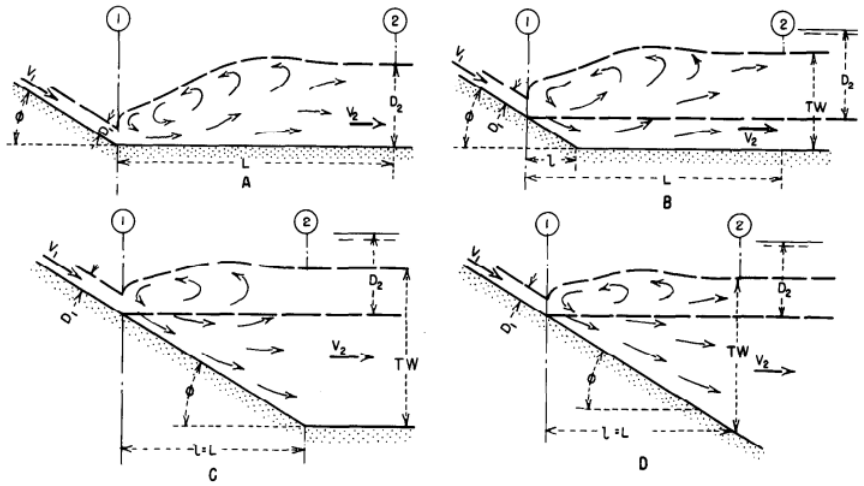

FIGURE 30.—*Sloping aprons (Basin V).*

Figure 4.5 Illustrative sketches made by Peterka (1958) for sloping apron.

Discharge values obtained from the simulations were given in the Table 4.2

Table 4.2 Average discharges values for 3 different chute channel angles

30˚ Chute channel angle	12.66 m^3/s
20˚ Chute channel angle	11.79 m^3/s
10˚ Chute channel angle	11.58 m^3/s

Different broad crested weir heights were tested to avoid sloping apron and starting point of the jump is observed. As the 60 cm cubic elements push the jump towards chute channel more, 60 cm cubic roughness elements were tested in this 3 simulations for 20˚ chute channel. Hydraulic jump locations were shared in Figure 4.6, Figure 4.7 and Figure 4.8 for the 1.32, 1.20 and 0.9-meter broad crested weir heights.

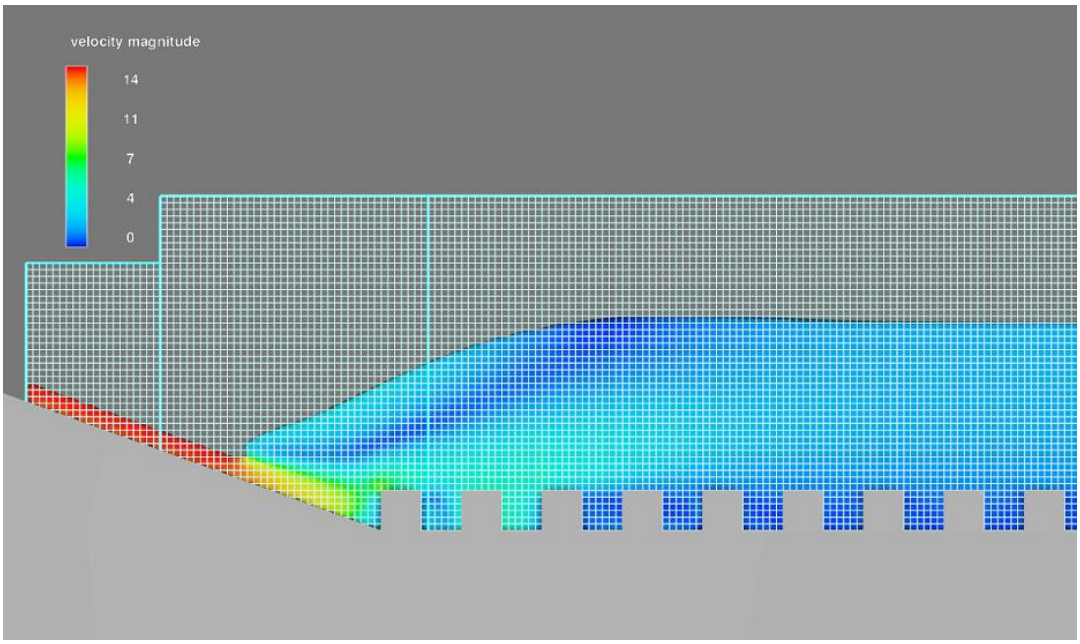

Figure 4.6 Hydraulic jump 2 meter away from the end of the chute channel for broad crested weir height is 1.32 meter

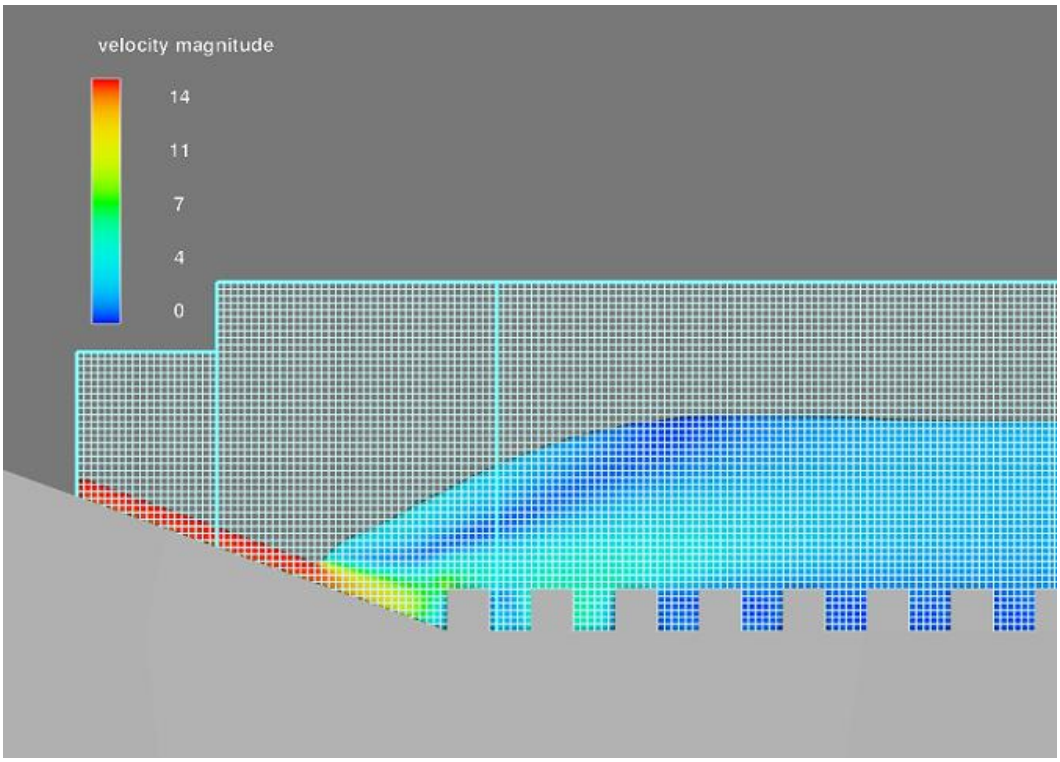

Figure 4.7 Hydraulic jump 1.8 meter away from the end of the chute channel for broad crested weir height is 1.20 meter

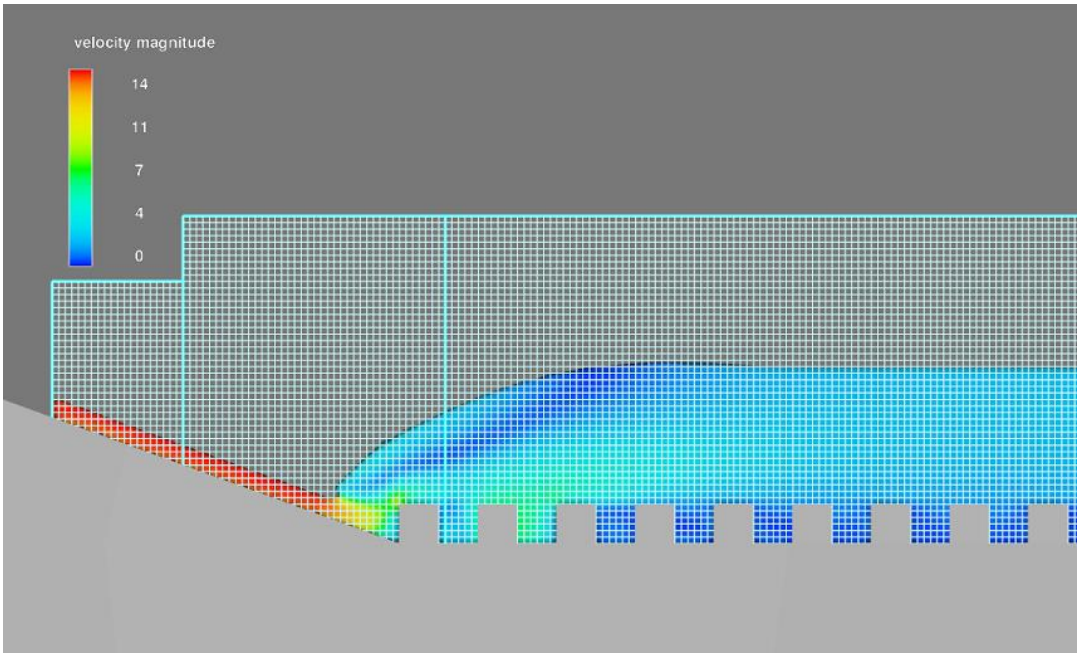

Figure 4.8 Hydraulic jump 1 meter away from the end of the chute channel broad crested weir height is 0.90 meter

As expected, when the tailwater depth increases, hydraulic jump forms at a location further upstream on the chute channel.After this test, simulations were carried out for 0.2, 0.3 and 0.4 meter size cubic roughness elements for the broad crested weir height of 0.9 meter. Hydraulic jumps occured in these cases were shared in Figure 4.9, Figure 4.10 and Figure 4.11 seperately.

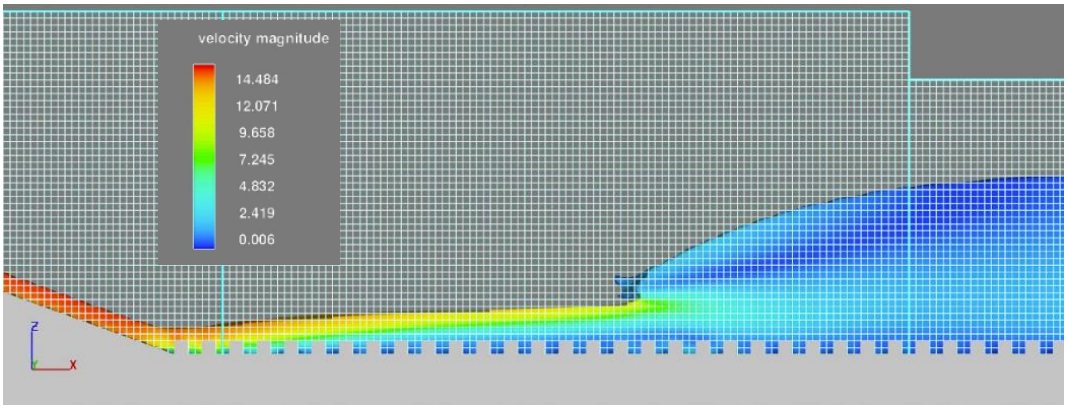

Figure 4.9 Hydraulic jump for 20˚ chute channel, 0.2 meter cubic elements size and 0.90 meter broad crested weir height

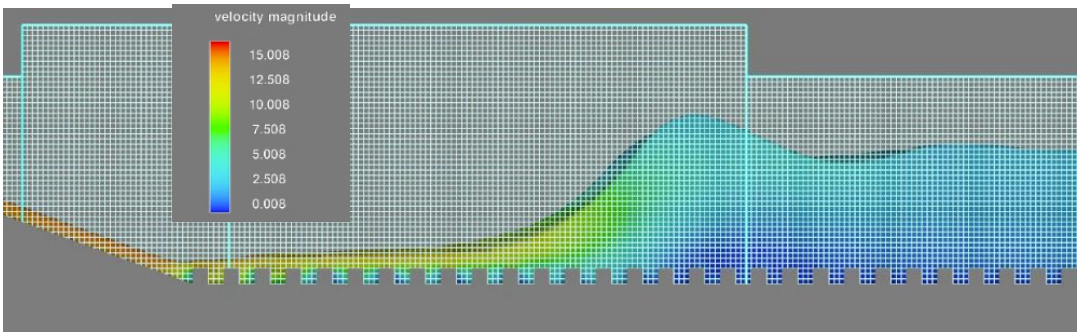

Figure 4.10 Hydraulic jump for 20˚ chute channel, 0.3 meter cubic elements size and 0.90 meter broad crested weir height

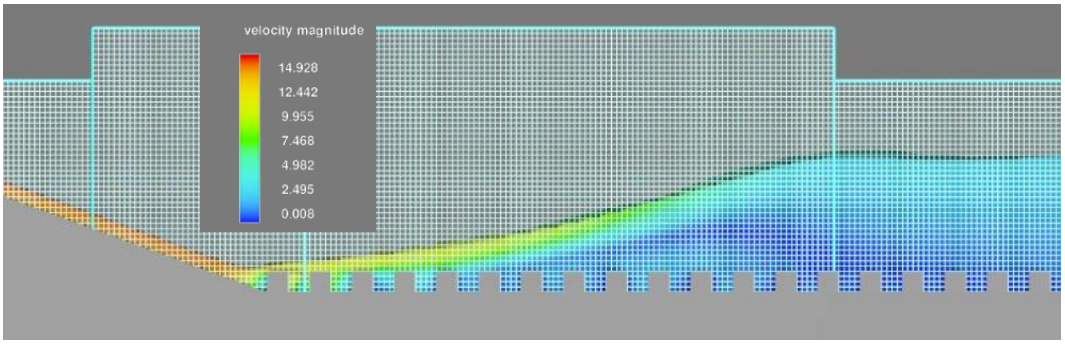

Figure 4.11 Hydraulic jump for 20˚ chute channel, 0.4 meter cubic elements size and 0.90 meter broad crested weir height

The results of simulations were interpreted as blocks' size change the formation shape of the hydraulic jump. As it seen in Figures some oscillations occurred on the surface of the water for 0.3-meter size cubic elements while water surface follows approximately a parabolic curve for 0.2-meter size cubic elements. On the other hand, water surface follows almost a linear line for 0.4-meter size cubic elements

The design is changed to see effect of starting point of roughness elements over the stilling basin and first 3 meters from the end of the chute channel is passed without macro roughness elements. This second design is already mentioned and shown in Figure 3.10.

When the simulations are solved for 0.2 meter cubic elements with a broad crested weir height of 1.2 meter, it was clear that hydraulic jump just started at the end of the chute channel as shown in Figure 4.12.

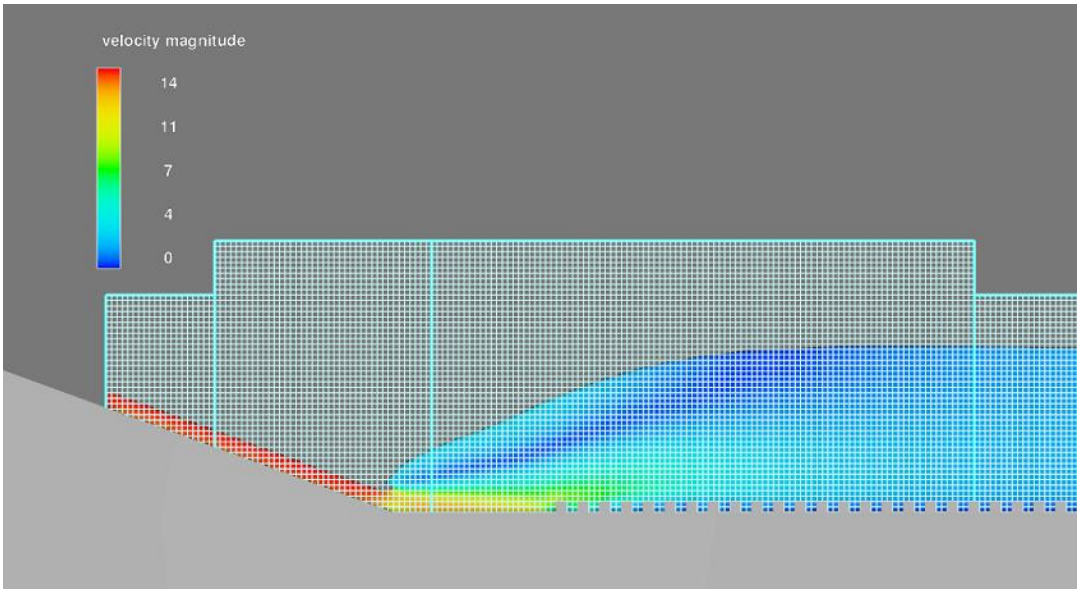

Figure 4.12 Hydraulic jump for 2 meter cubic elements for broad crested weir height of 1.2 meter with 3 a meter block-free surface.

When the simulation is solved under the same conditions for 0.2 meter cubic elements without block-free surface, Figure 4.13 is obtained. As it seen from that figure hydraulic jumps started 0.7 meter earlier with respect to "3 meter blocks-free surface" case.

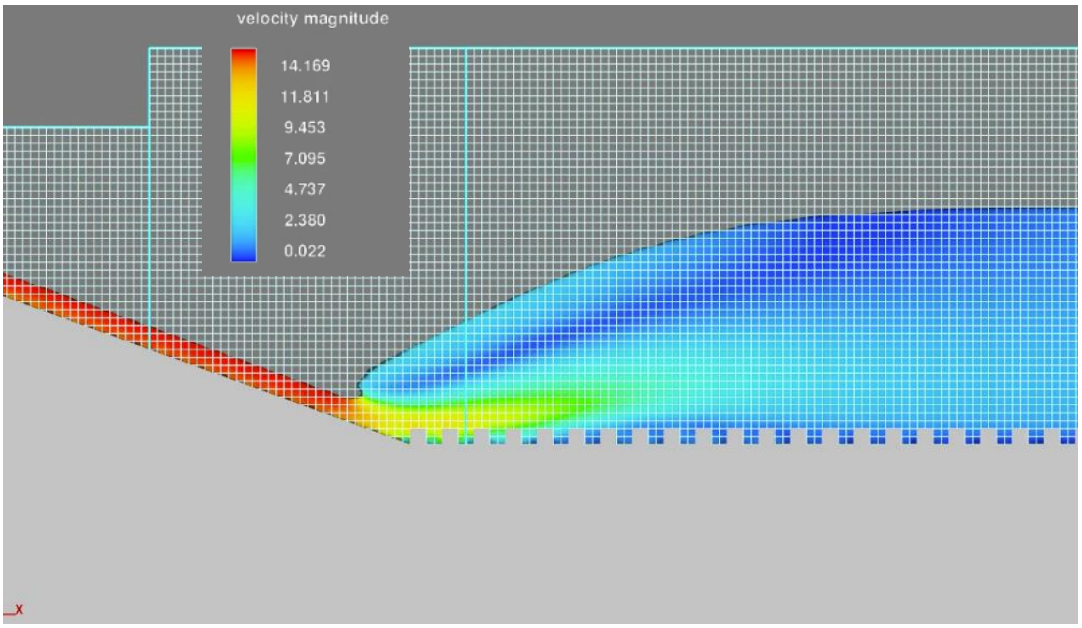

Figure 4.13 Hydraulic jump for 2 meter cubic elements for broad crested weir height of 1.2 meter without blocks-free surface.

Also, hydraulic jump length is affected from the starting point of roughness elements over the stilling basin. Hydraulic jump length increases with block free surfaces. Jump lengths values for these two cases are compared in Table 4.3.

Table 4.3 Hydarulic jump length comparison of 3 meter blocks free surface with fully equipped surface

	X Coordinate for y_1 (m)	**X Coordinate for y_2(m)**	**Jump Length (m)**
0.2 meter cubic roughness elements without block-free surface. (Fully equipped surface)	143.59	150.88	7.29
0.2 meter cubic roughness elements with 3 meter block-free surface.	144.29	152.20	7.91

Broad crested weir height was dropped to 0.5 meter to see the formation of the hydraulic jump over stilling basin for other roughness elements sizes with 3-meter block-free surface. Hydraulic jump is seen at the stilling basin as it shown in Figure

4.14 for case which has 0.5-meter height of broad crested weir and 0.2-meter size roughness elements.

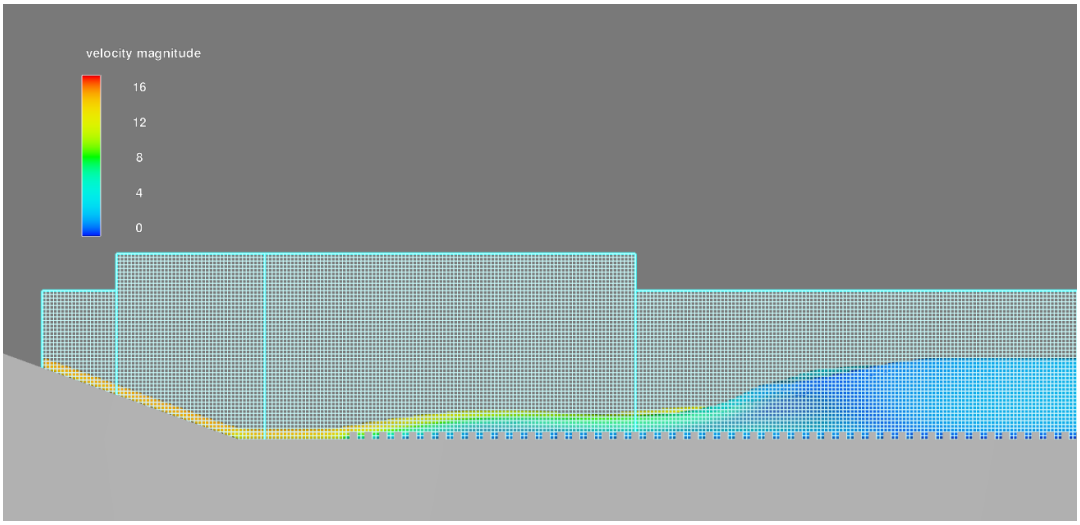

Figure 4.14 Hydraulic jump when the broad crested weir height is 0.5 meter and the stilling basin has 0.2 meter cubic roughness elements

Then, the model which are equipped with 0.3, 0.4 and 0.5 meter cubic elements were tested for broad crested weir height of 0.5 meter. Formation of the hydraulic jump for 0.4 meter cubic elements is shown in Figure 4.15.

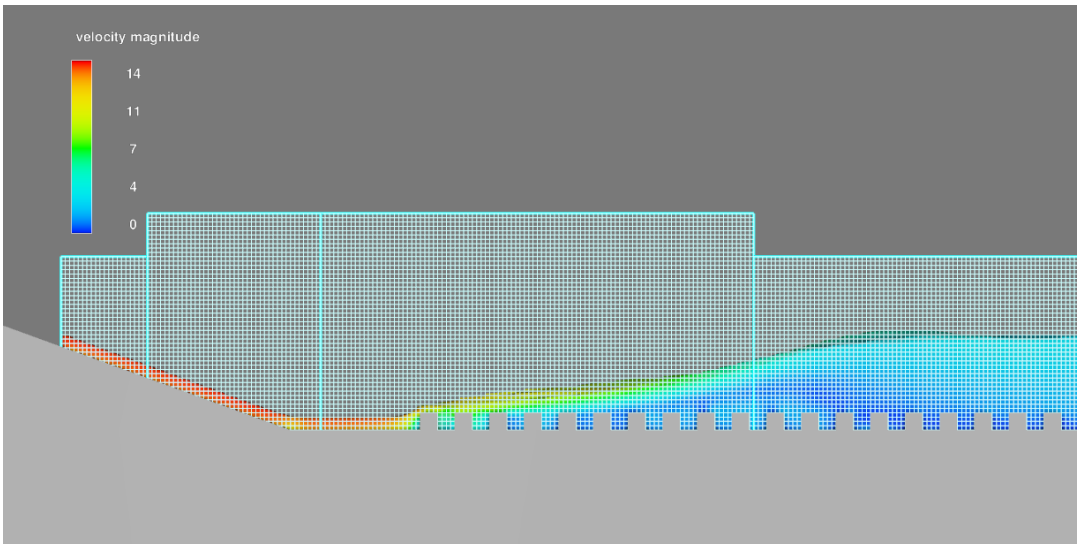

Figure 4.15 Hydraulic jump when the broad crested weir height is 0.5 meter and the stilling basin has 0.4 meter cubic roughness elements

When the simulation is solved for 0.5-meter cubic roughness element size, water splashes as it seen from figure 4.16. It looks like that when the size of the cubic elements gets closer to the critical flow depth, splashes occurred and formation of the hydraulic jump could not be observed properly according to jump forms specified by Peterka (1958).

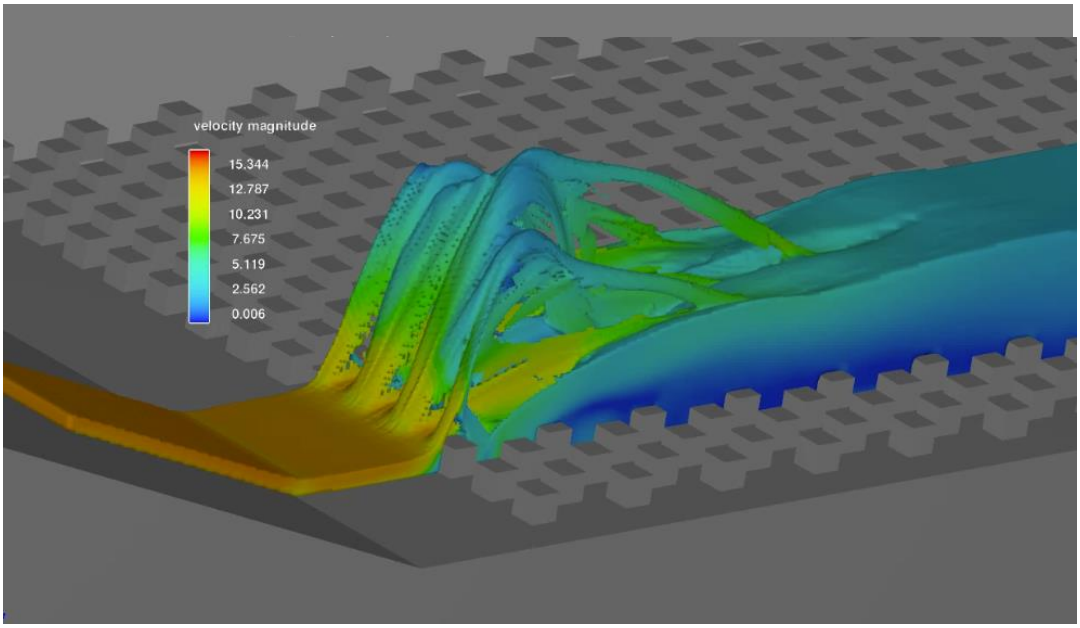

Figure 4.16 Water splashes when the broad crested weir height is 0.5 meter and the stilling basin has 0.5 meter cubic roughness elements

4.1.1 Results in Chute Channel and Broad Crested Weir

For 30 degree chute channel the discharge value is recorded from the simulations. For different broad crested weir height y_{2s} values were calcuated from conservation of energy. Then, y_1 values were calculated with using Belanger equation. To control the flow depth, P=1.67 m height broad crested weir is added to stilling basin. These procedure was mentioned in the introduction part. Pysical values for flow are shared in Figure 4.17.

q(taken from the simulation): 4.22 m³/s/m

$$y_c = \sqrt[3]{\frac{q^2}{g}} = \sqrt[3]{\frac{4.22^2}{9.81}} = 1.22m$$

$$1.67 = y_{2s} - y_c + \frac{q^2}{y_{2s}^2 \times 2g} - \frac{q^2}{y_c^2 \times 2g}$$

$$y_{2s} = 3.42\ m$$

q	=	4.22	m³/s/m
y_{2s}	=	3.42	m
y_c	=	1.22	m
V_{2s}	=	1.23	m/s
V_c	=	3.46	m/s
E_2	=	3.50	
E_c	=	1.83	
P	=	1.67	m

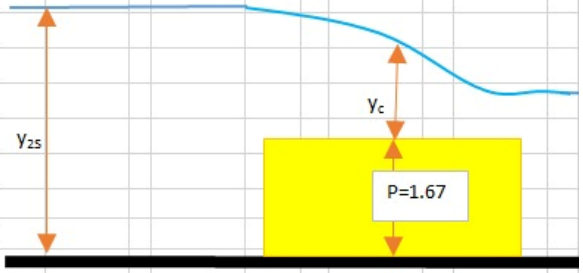

Figure 4.17 Broad crested weir for 30° Chute channel.

This procedure is completed for other cases which were used in the study as well. Pysical values for flow and design value of the broad crested weir were shared for 10° chute channel angle and broad crested weir height of 1.58 meter & 20° chute channel angle and broad crested weir height of 1.2 meter in Figure 4.18 and 4.19.

q	=	3.93	m³/s/m
y_{2s}	=	3.25	m
y_c	=	1.16	m
V_{2s}	=	1.21	m/s
V_c	=	3.38	m/s
E_2	=	3.33	
E_c	=	1.74	
P	=	1.58	m

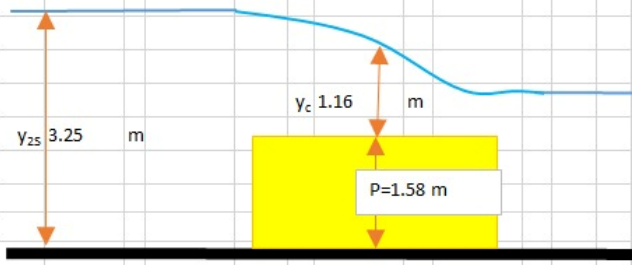

Figure 4.18 Broad crested weir for 20° Chute channel.

q	=	3.86	m³/s/m
y_{2s}	=	2.83	m
y_c	=	1.15	m
V_{2s}	=	1.36	m/s
V_c	=	3.36	m/s
E_{2s}	=	2.92	
E_c	=	1.72	
P	=	1.20	m

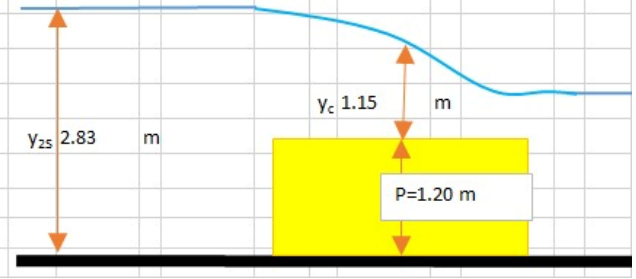

Figure 4.19 Broad crested weir for 10° chute channel.

General view and physical quantities is shown for 20° chute channel angle and 0.50 meter height broad crested weir in Figure 4.20.

q(taken from the simulation): 3.93 m³/s/m

$$y_c = \sqrt[3]{\frac{q^2}{g}} = \sqrt[3]{\frac{3.93^2}{9.81}} = 1.16m$$

$$0.5 = y_{2s} - y_c + \frac{q^2}{y_{2s}^2 \times 2g} - \frac{q^2}{y_c^2 \times 2g}$$

$$y_{2s} = 2.07\ m$$

q	=	3,93	m³/s/m
y_{2S}	=	2,07	m
y_c	=	1,16	m
V_{2S}	=	1,90	m/s
V_c	=	3,38	m/s
E_{2S}	=	2,25	
E_2	=	1,75	
P	=	0,50	m

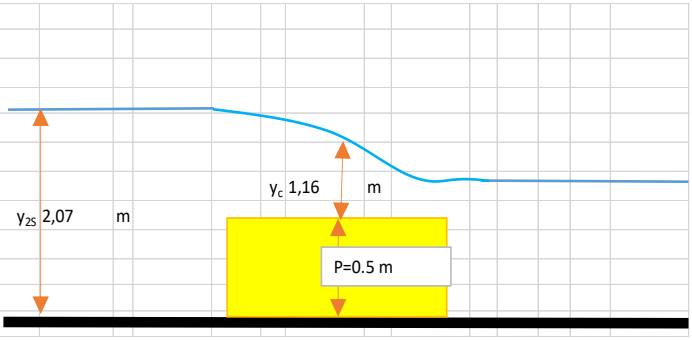

Figure 4.20 . General view and physical quantities for 20° angle chute channel angle and 0.5 meter height broad crested weir

From downstream with using Belanger equation y_1 value is found.

$$Fr_2 = \frac{V_2}{\sqrt{gy_2}} = \frac{1.90}{\sqrt{9.81x2.07}} = 0.42$$

$$y_1 = \frac{y_2}{2}(-1+\sqrt{1+8\times Fr_2^2})$$

$y_1 = \frac{2.07}{2}(-1+\sqrt{1+8\times 0.42^2} = 0.57$ mThen Fr_1 = 2.07, important physical values are shown in Table 4.4 for 0.5-meter broad crested weir.

Table 4.4 Flow physical quantities for 0.5 meter broad crested weir

q	3.93	m³/s/m
B	3.00	m
Q	11.79	m³/s
g	9.81	m/s²
yc	1.16	m
α	20.00	Degree
y_1	0.57	
V_1 (m/s)	6.84	m/s
Fr_1	2.88	
y_{2S}	2.07	m

General view and physical quantities is shown for 20° chute channel angle and 0.90 meter height broad crested weir in Figure 4.21.

q(taken from the simulation): 3.93 m³/s/m

$$y_c = \sqrt[3]{\frac{q^2}{g}} = \sqrt[3]{\frac{3.93^2}{9.81}} = 1.16m$$

$$0.9 = y_{2s} - y_c + \frac{q^2}{y_{2s}^2 \times 2g} - \frac{q^2}{y_c^2 \times 2g}$$

$$y_{2s} = 2.53\ m$$

q	=	3.93	m³/s/m
y_{2S}	=	2.53	m
y_c	=	1.16	m
V_{2s}	=	1.56	m/s
V_c	=	3.38	m/s
E_{2s}	=	2.65	
E_2	=	1.75	
P	=	0.90	m

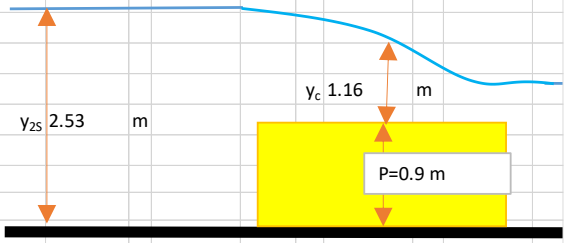

Figure 4.21 General view and physical quantities for 20° angle chute channel and 0.9 meter height broad crested weir

From downstream with using Belanger equation y_1 value is found.

$$Fr_2 = \frac{V_2}{\sqrt{gy_2}} = \frac{1.56}{\sqrt{9.81x2.53}} = 0.31$$

$$y_1 = \frac{y_2}{2}(-1+\sqrt{1 + 8 \times Fr_2^2})$$

$y_1 = \frac{2.53}{2}(-1 + \sqrt{1 + 8 \times 0.31^2} = 0.42$ m Then Fr_1 = 2.95, important physical values are shown in Table 4.5 for 0.9-meter broad crested weir.

Table 4.5 Flow physical quantities for 0.9 meter broad crested weir

q	3.93	$m^3/s/m$
B	3.00	m
Q	11.79	m^3/s
g	9.81	m/s^2
yc	1.16	m
α	20.00	Degree
y_1	0.42	
V_1 (m/s)	9.33	m/s
Fr_1	4.59	
y_{2S}	2.53	m

4.1.2 Results in the Stilling Basins

As the tailwater depth is fixed with a broad-crested weir, change in energy head will be so close to each other for different stilling basins at the same length. Because of that, focusing on hydraulic jump length is a more accurate way to see energy dissipation efficiency. Therefore, jump lengths show the effectiveness of the macro roughness elements.

For the stilling basin according to x coordinates obtained depth of the flow and velocity, Froude number, energy head values were calculated. To see difference in Hydraulic Jumps' formation with respect to stilling basin types, Flow Depth vs x coordinate graphs are drawn and shown in Figure 4.22, Figure 4.24, and Figure 4.26 for 30 degrees for broad crested weir height of 1.67 meter, 20 degrees for broad crested weir height of 1.58 meter and 10-degree chute channels for broad crested weir height of 1.20 meter cases, respectively.

Z coordinate vs x coordinate graphs of the flow are shown in Figure 4.23, Figure 4.25, and Figure 4.27 for 30 degrees for broad crested weir height of 1.67 meter, 20 degrees for broad crested weir height of 1.58 meter and 10-degree chute channels for broad crested weir height of 1.20 meter cases, respectively.

The zero point of the x coordinate is at the starting point of the reservoir. Since the length of the chute channel changes according to the angle of the channel, the starting point of the stilling basin also changes. The starting point x-coordinate of the stilling basin at different angles are given in Table 4.6.

Table 4.6 The starting point of stilling basin with respect to chute channel angle.

Chute channel angle (degrees)	X-coordinate of the Starting point of stilling basin (m)
30	98.76
20	144.29
10	275.73

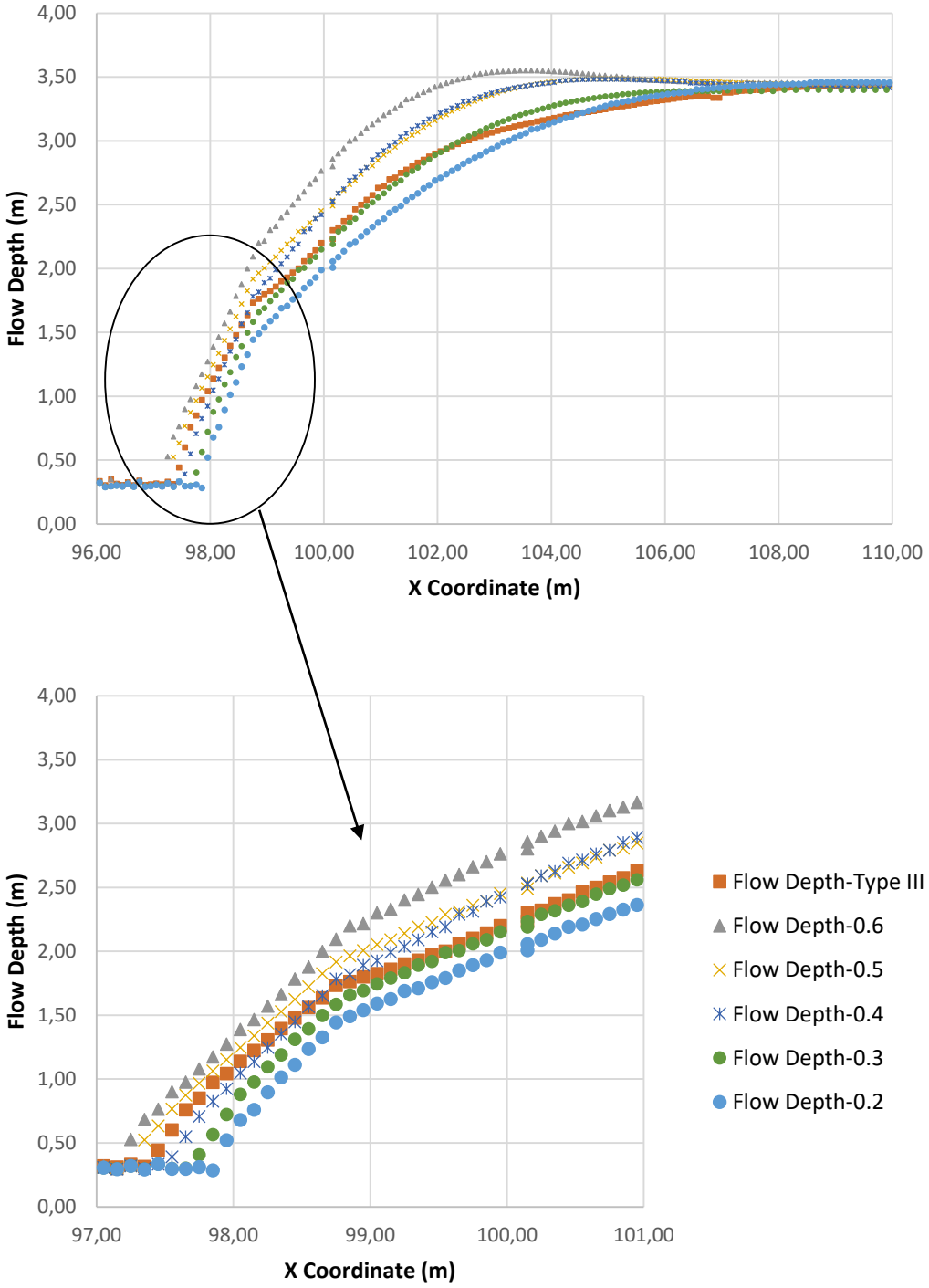

Figure 4.22 Flow depth graph for 30 degree chute channel and broad crested weir height of 1.67 meter

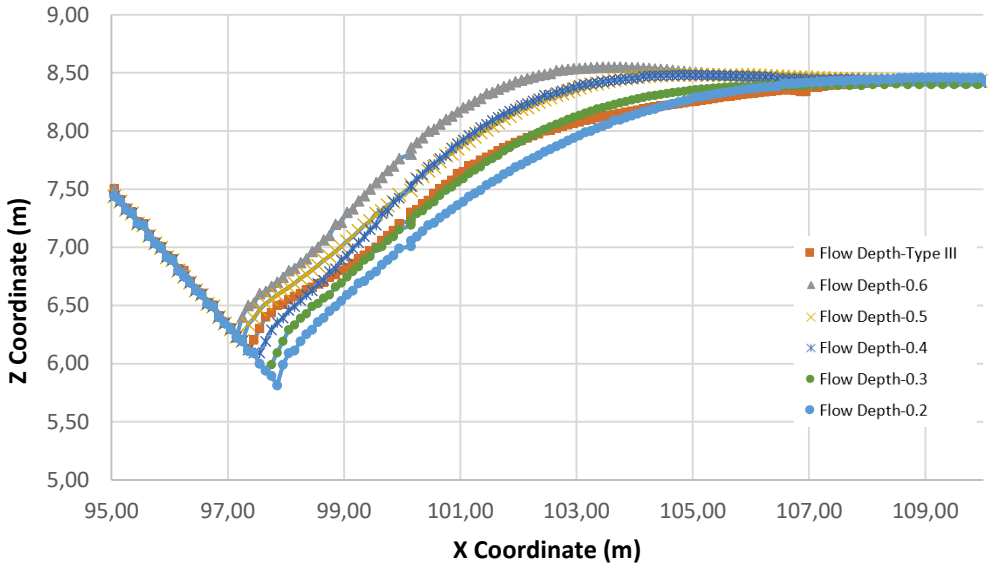

Figure 4.23 Flow profile at z-x coordinate system for 30-degree chute channel and broad crested weir height of 1.67 meter

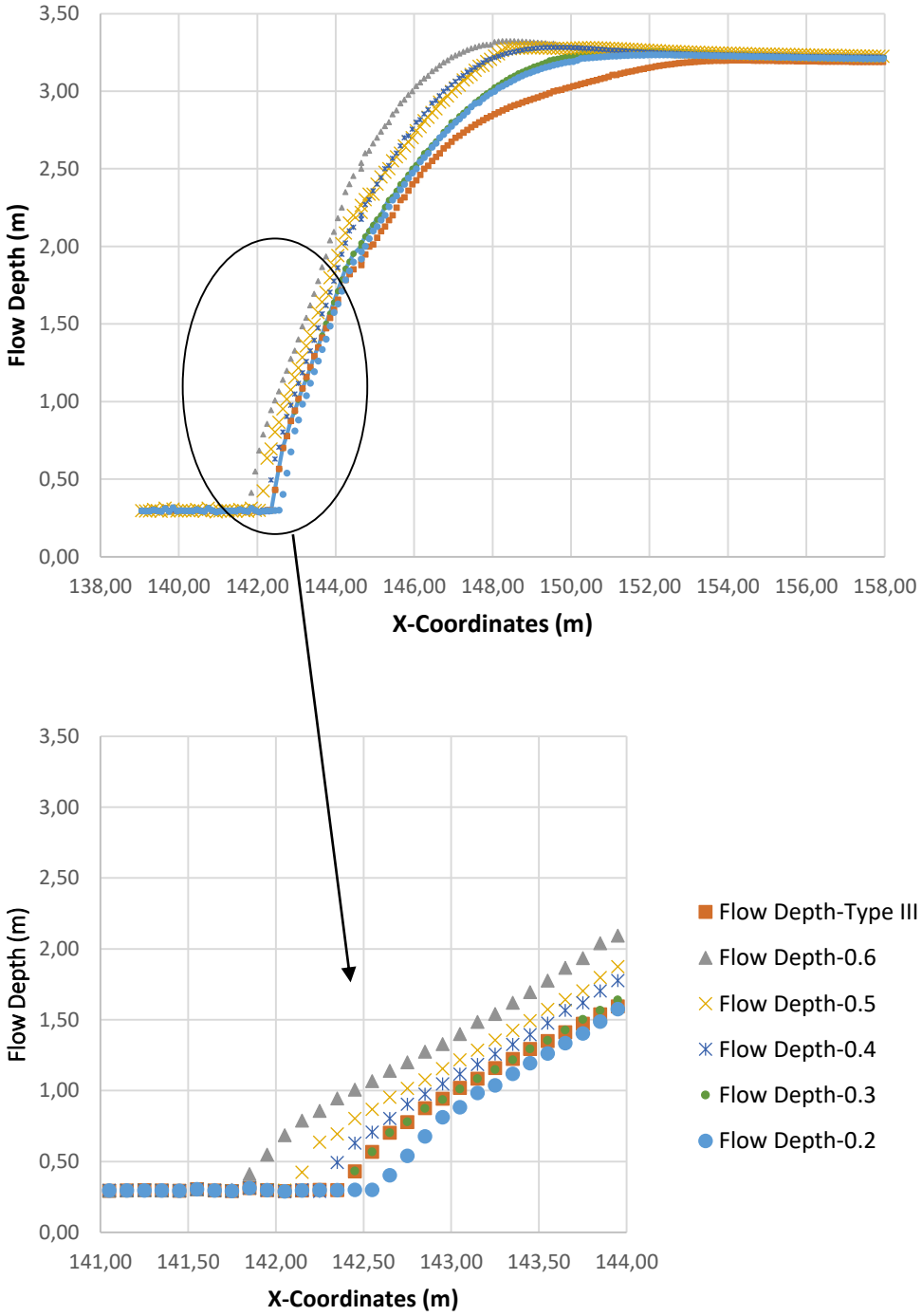

Figure 4.24 Flow depth graph for 20 degree chute channel and broad crested weir height of 1.58 meter

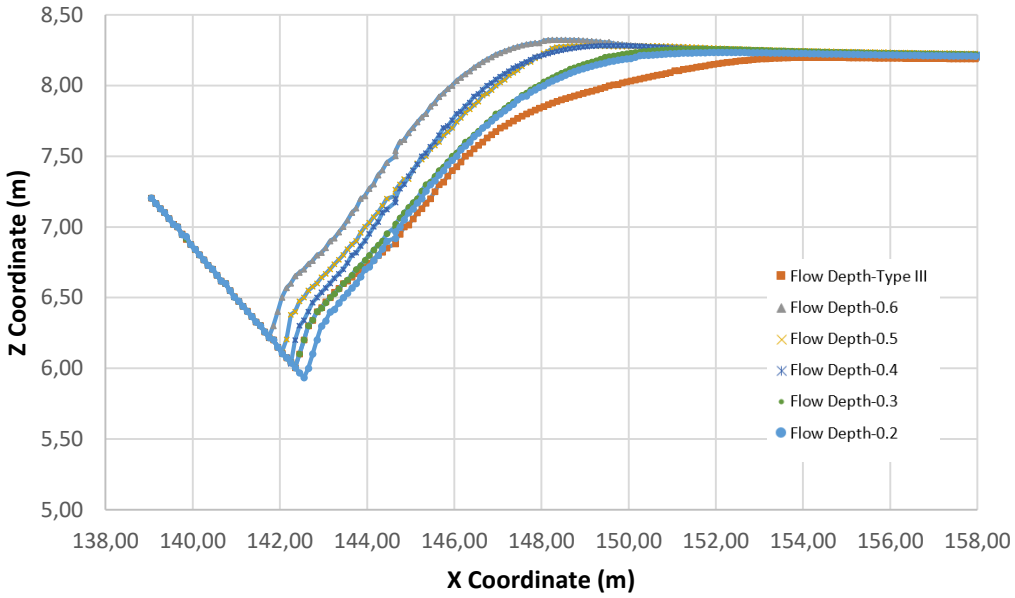

Figure 4.25 Flow profile at z-x coordinate system for 20 degree chute channel and broad crested weir height of 1.58 meter

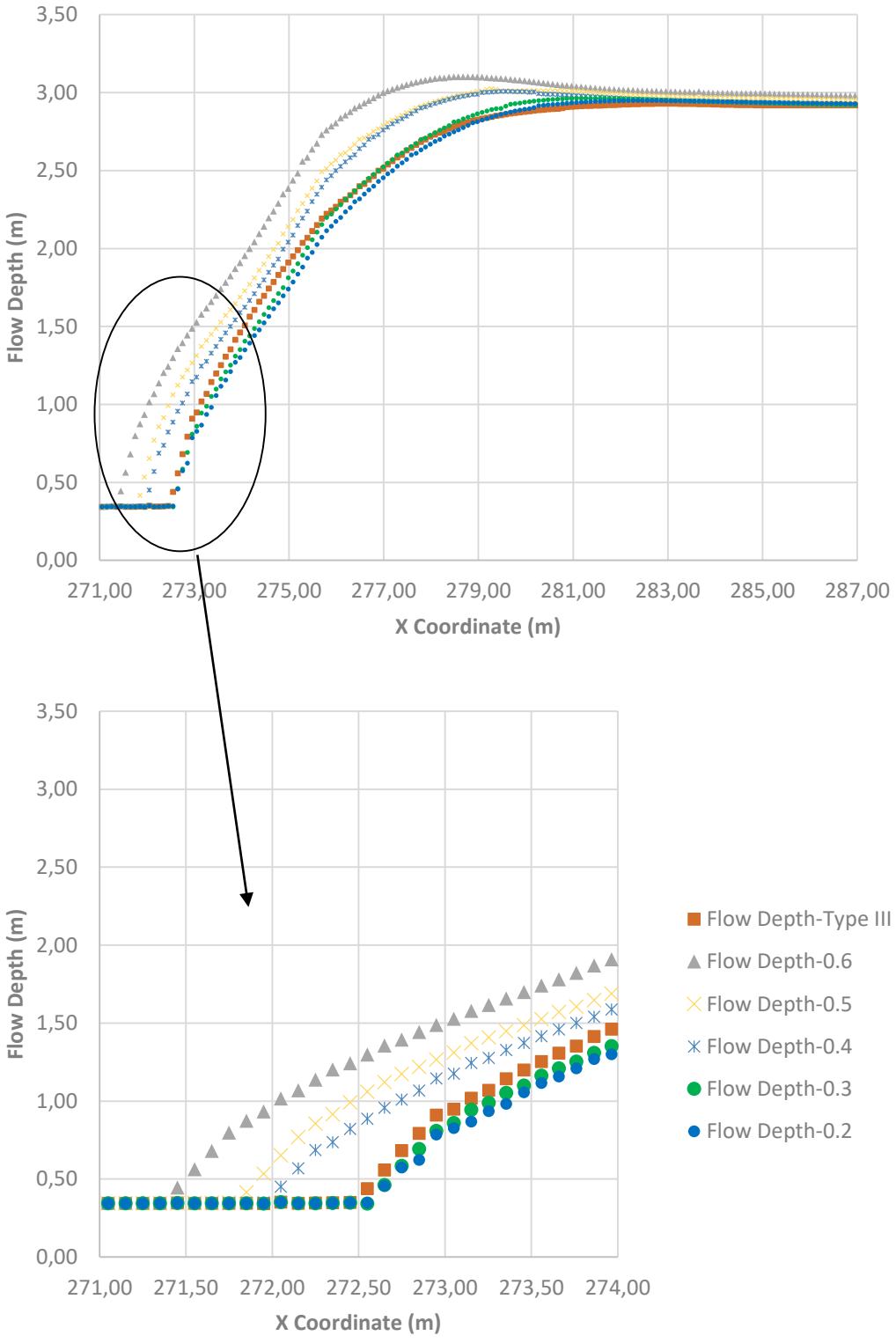

Figure 4.26 Flow depth graph for 10 degree chute channel and broad crested weir height of 1.20 meter

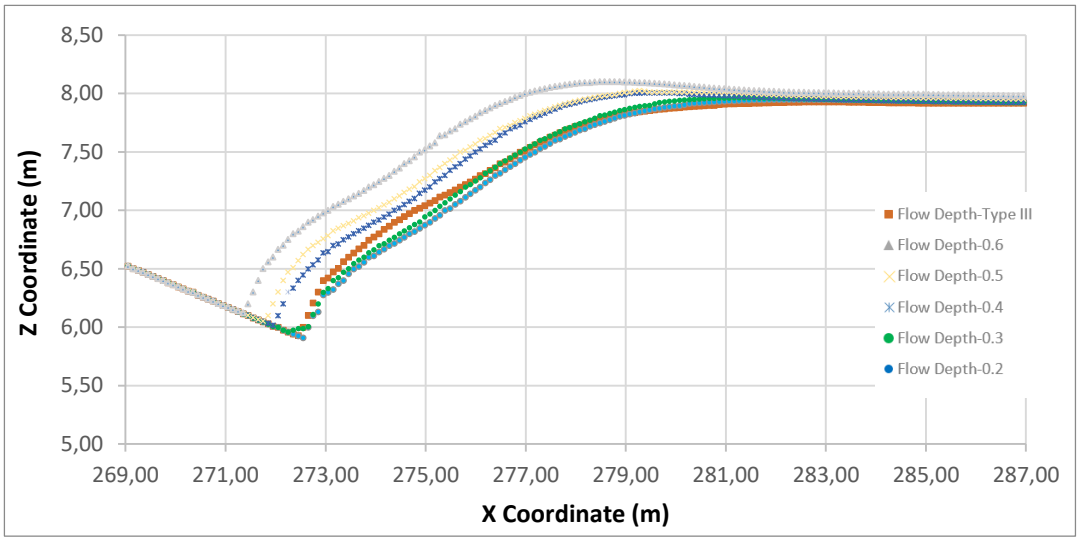

Figure 4.27 Flow profile at z-x coordinate system for 10 degree chute channel and broad crested weir height of 1.20 meter

As it can be understood from these figures, the starting point of hydraulic jumps which is shown in Figure 4.28 is delayed as the size of the cubic elements gets smaller.

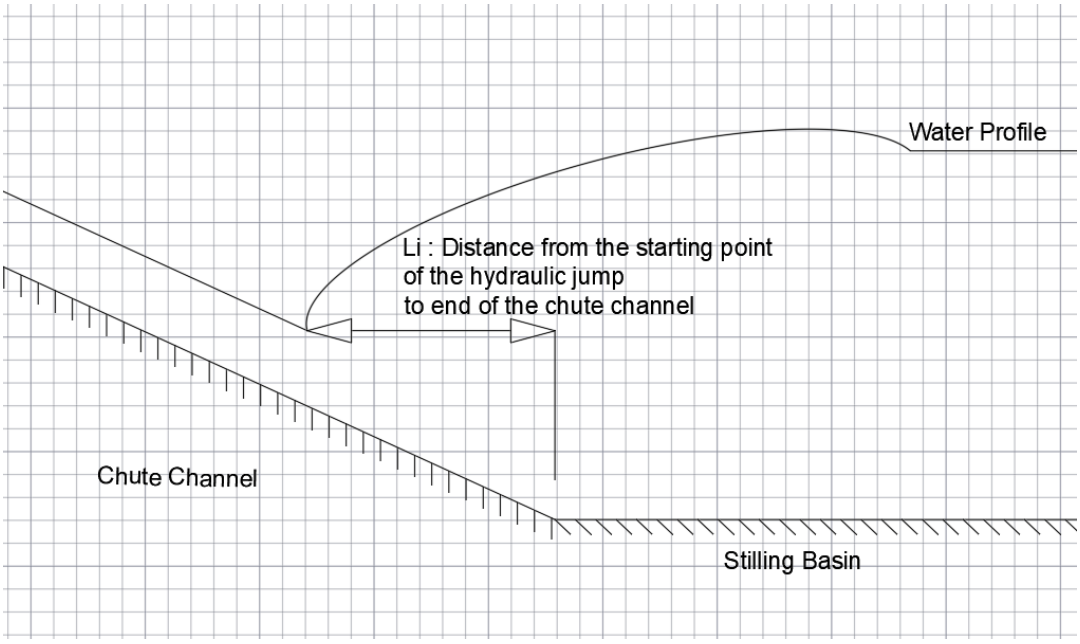

Figure 4.28 Distance from the starting point of the hydraulicto end of the chute channel (Li)

For US Type III Design, it is observed that the hydraulic jump pattern falls between cases with 50 cm and 30 cm cubic elements in the stilling basin. The distance from the starting point of the hydraulic jump to the end point of the chute channel (Li) increases in direct proportion to the increase in the dimensions of the cubic elements used as it is seen from Figure 4.29.

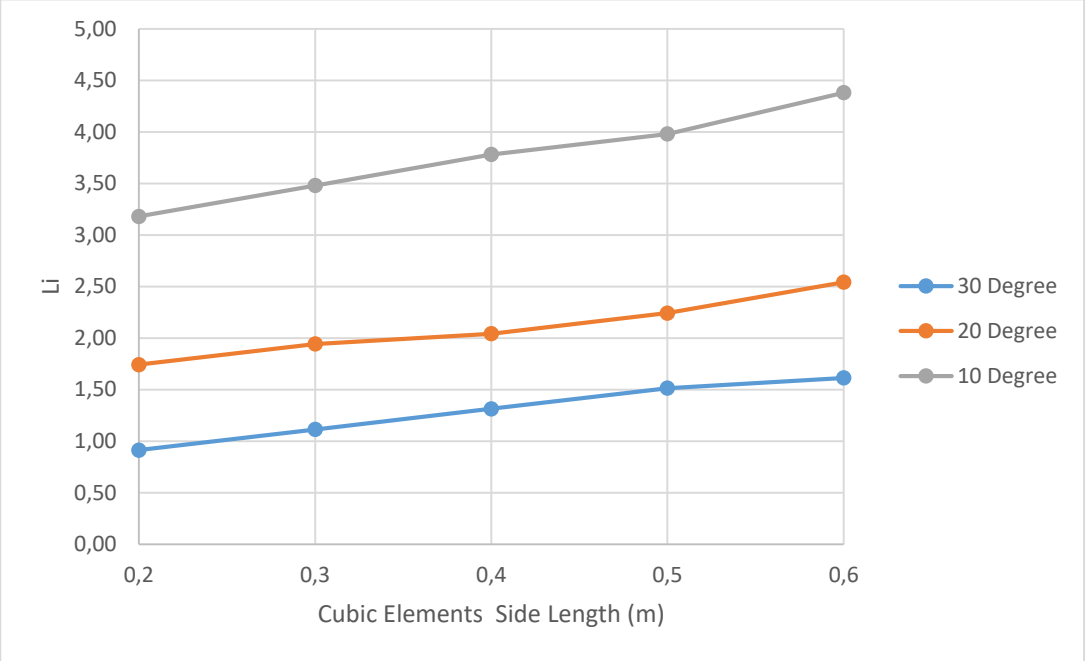

Figure 4.29 Distance from the starting point of the jump to the end of the chute channel vs cubic elements side length

Δx is the change in the cubic element side length. The relationship between the change in the dimensions of the cubic elements and change in the translation amount (Δl) of the hydraulic jump is given in equations (9) and (10) for chute channels with 20̊-30̊ and 10̊ slope respectively. (Between the side length range of 0.2 m to 0.6 m).

For 20̊ & 30̊ Chute Channel;

$$\Delta l \cong 2 \times \Delta x \tag{9}$$

For 10̊ Chute Channel;

$$\Delta l \cong 3 \times \Delta x \tag{10}$$

In the US design, distance from the starting point of the hydraulic jump to the starting point of the chute channel (Li) is similar to the other models with cubic elements.

For the chute channel angle of 30, the designs made with cubic element size of 50 cm and above shift the hydraulic jump towards the chute channel more than the US design. For 20° and 10° angles, designs made with 30 cm or larger size cubic elements shift the hydraulic jump towards the chute channel more than the US design.

As the chute angle decreases, the cubic elements push the hydraulic jump towards chute channel more efficiently with respect to US Design. Such that, at an angle of 10, the offset difference between the 60 cm cubic design and the US design reaches up to a meter. A comparison of the two designs are given in Table 4.7.

Table 4.7 Comparison of Li values from simulations of 60 cm cubic elements and the US Design for different chute channel angles.

Angle of the Chute Channel	Distance from the starting point of the jump to end of the chute channel		Difference (m)
	US Design (m)	60 cm Cubic Elements (m)	
30	1.41	1.61	0.20
20	1.94	2.54	0.60
10	3.28	4.38	1.10

Distance from the starting point of the jump to end of the chute channel (Li) values for different simulations are shown in Table 4.8.

Table 4.8 Distance from the starting point of the jump to end of the chute channel (Li)

Froude Number:	**7.75**	**Type Of The Stilling Basin**	**End Of the Chute Channel (m)**	**Jump Starting Point (m)**	**Li (m)**
30	**Degree**	Type III	98.76	97.35	1.41
Broad Crested Weir Height:1.67 meter		0.2	98.76	97.85	0.91
		0.3	98.76	97.65	1.11
		0.4	98.76	97.45	1.31
		0.5	98.76	97.25	1.51
		0.6	98.76	97.15	1.61
Froude Number:	**7.60**	**Type Of The Stilling Basin**	**End Of the Chute Channel**	**Jump Starting Point**	**Li**
20	**Degree**	Type III	144.29	142.35	1.94
Broad Crested Weir Height:1.58 meter		0.2	144.29	142.55	1.74
		0.3	144.29	142.35	1.94
		0.4	144.29	142.25	2.04
		0.5	144.29	142.05	2.24
		0.6	144.29	141.75	2.54
Froude Number:	**6.05**	**Type Of The Stilling Basin**	**End Of the Chute Channel**	**Jump Starting Point**	**Li**
10	**Degree**	Type III	275.73	272.45	3.28
Broad Crested Weir Height:1.20 meter		0.2	275.73	272.55	3.18
		0.3	275.73	272.25	3.48
		0.4	275.73	271.95	3.78
		0.5	275.73	271.75	3.98
		0.6	275.73	271.35	4.38

Comparison of the hydraulic jump length is an important parameter for investigating the effect of energy dissipation for different cubic element sizes. Depth of flow values obtained from simulations were examined to calculate the hydraulic jump length. The incoming water depth was controlled by data taken every 10 cm, and the location where the dramatic increase existed was accepted as the starting point for the hydraulic jump. Using the data taken every 10 cm in the flow direction, the point where the water height is maximum is accepted as the point where the hydraulic jump ends.

Obtained results from the simulations are shared in Table 4.9. As can be seen from this table, the length of hydraulic jumps decreases as the size of the cubic elements gets bigger. In all the scenarios tested, the hydraulic jump lengths in the stilling basin formed with cubic elements are shorter than the hydraulic jump forming in the US design stilling basin.

Table 4.9 The Length of the Hydraulic Jumps

Froude Number: 7.75	Design Type	Jump Starting Point (m)	The Point where The Flow Depth Reaches Max. Level (m)	Jump Length (m)
30 Degree	Type III	97.35	111.05	13.70
Broad Crested Weir Height:1.67 meter	0.2	97.85	109.15	11.30
	0.3	97.65	108.50	10.85
	0.4	97.45	105.25	7.80
	0.5	97.25	104.95	7.70
	0.6	97.15	103.55	6.40
Froude Number: 7.60	Design Type			Jump Length
20 Degree	Type III	142.35	154.25	11.90
Broad Crested Weir Height:1.58 meter	0.2	142.55	152.15	9.60
	0.3	142.35	151.55	9.20
	0.4	142.25	149.55	7.30
	0.5	142.05	148.95	6.90
	0.6	141.75	148.35	6.60
Froude Number: 6.05	Design Type			Jump Length
10 Degree	Type III	272.45	282.96	10.51
Broad Crested Weir Height:1.20 meter	0.2	272.55	282.46	9.91
	0.3	272.25	281.37	9.12
	0.4	271.95	279.57	7.62
	0.5	271.75	279.27	7.52
	0.6	271.35	278.68	7.33

When Table 4.9 is examined, one can conclude that for all the chute slopes tested the size of the hydraulic jump decreases as the size of the cubic blocks increase. Simulation results for the US design scenario and the theoretical values for the hydraulic jump lengths were also checked for the reliability of the study.

There are some empirical relationships based on experimental data which are made by US Bureau of Reclamation. They (1955) developed a chart that took into account the relationship between length ratio and upstream Froude number which is shown in Figure 4.19. L refers hydraulic jump length in the figure while D_2 is tailwater depth which is y_2 in this study.

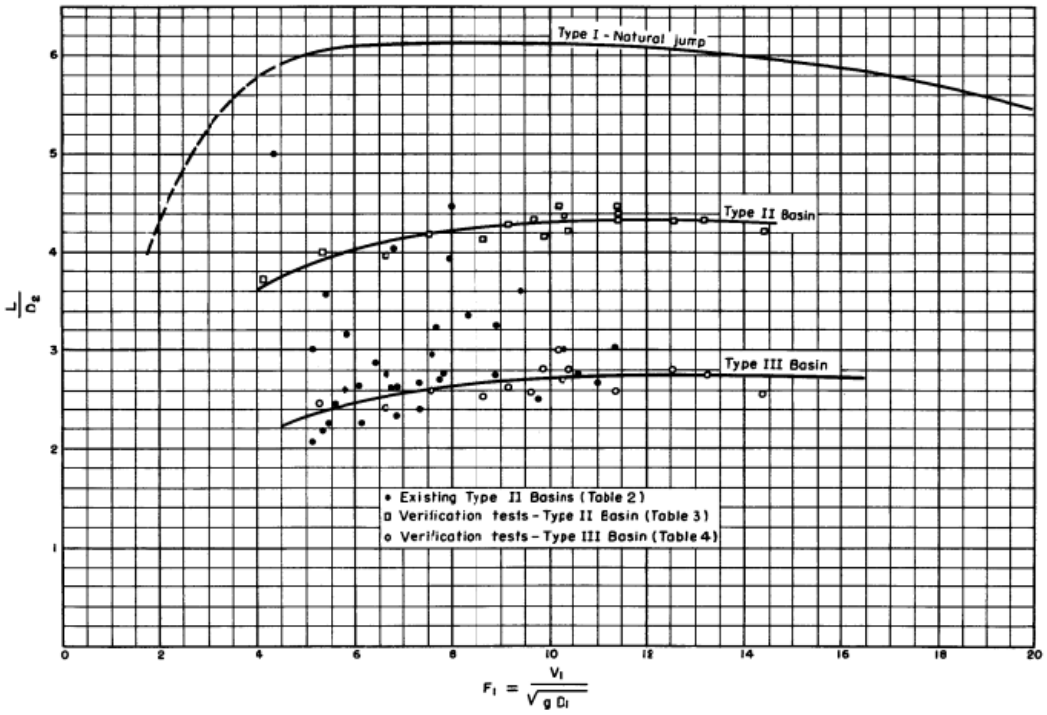

Figure 4.30 Length of jump on the horizontal floor

The hydraulic jump lengths that will occur under normal conditions can be approximated by Chow's equation.

The related Formula is given as (Chow, 1959)

$$L_j = 6.1y_2 \tag{11}$$

For 30̊ angle & Broad Crested weir height is 1.67 case;

$y_2 = 3.42$ => $L_j = 6.1y_2$ =20.86 m

For 20̊ angle & Broad Crested weir height is 0.5 case;

$y_2 = 2.07\ meter$ => $L_j = 6.1y_2$ =12.63 meter

For 20̊ angle & Broad Crested weir height is 0.9 case;

$y_2 = 2.53\ meter$ => $L_j = 6.1y_2$ =15.43 meter Normal hydraulic jump lengths are less than the hydraulic jump lengths obtained from the simulations which is solved with cubic roughness elements. This shows that cubic roughness elements used in the stilling basin are useful in decreasing the length of the hydraulic jump.

For the US Design model with 30̊ angle chute channel, theoretical length of the jump is calculated as 10.26 m for which the corresponding value is calculated as 13.7 m in this study. This 33% difference is a bit high. This might be related to the insufficient turbulent energy dissipation in the numerical model. In the numerical study air entrainment is ignored and this might have resulted in this large difference in the hydraulic jump length. If air entrainment was provided, energy dissipation would increase due to turbulent flow and the hydraulic jump length would be shortened. In this case, the values could converge to the USBR values, enabling us to reach more accurate results. However, the air-entrainment model in the code has to be tuned up before using as it uses some empirical relationships.

As the angle in the chute channel increases, more effective energy dissipation is observed for 40 cm, 50 cm and 60 cm cubic elements as the jump length decreases. Examining the rates of change in hydraulic jump length, current study can provide us information about the effective use of cubic elements. For this reason, percentage change in hydraulic jump length is calculated between the hydraulic jump length in the stilling basin formed with each cubic element and the hydraulic jump length in the stilling basin formed with US design. These values are given in Table 4.10 and Table 4.11.

Table 4.10 Percentage change in hydraulic jump length with respect to US design for each channel slope

Froude Number:	7.75		Jump Length (m)	Percent reduction with respect to US Design
30	Degree	Type III	13.70	-
Broad Crested Weir Height:1.67 meter		0.2	11.30	17.52%
		0.3	10.85	20.80%
		0.4	7.80	43.07%
		0.5	7.70	43.80%
		0.6	6.40	53.28%
Froude Number:	7.60		Jump Length (m)	Change percentage with respect to US Design
20	Degree	Type III	11.90	-
Broad Crested Weir Height:1.58 meter		0.2	9.60	19.33%
		0.3	9.20	22.69%
		0.4	7.30	38.66%
		0.5	6.90	42.02%
		0.6	6.60	44.54%
Froude Number:	6.05		Jump Length (m)	Change percentage with respect to US Design
10	Degree	Type III	10.51	-
Broad Crested Weir Height:1.20 meter		0.2	9.91	5.69%
		0.3	9.12	16.11%
		0.4	7.62	27.46%
		0.5	7.52	28.44%
		0.6	7.33	30.27%

Table 4.11 Percentage change and physical difference in hydraulic jump length with respect to US design for each cubic element size

		Cubic Elements Length (m)				
		0.6	0.5	0.4	0.3	0.2
		Percent reduction with respect to US design				
Chute Channel Angle	10	30.27%	28.44%	27.46%	16.11%	5.69%
	20	44.54%	42.02%	38.66%	22.69%	19.33%
	30	53.28%	43.80%	43.07%	20.80%	17.52%
		Change in Hydraulic Jump Length With Respect to Us Design (m)				
	10	3.18	2.99	2.89	1.39	0.60
	20	5.30	5.00	4.60	2.70	2.30
	30	7.30	6.00	5.90	2.85	2.40

Especially in stilling basins with 40, 50 and 60 cm cubic elements, the reduction in hydraulic jump length is more effective than the stilling basins made with 20 and 30 cm cubic elements. The trend of change in hydraulic jump length of cubic elements of different sizes as the angle of the chute channel changes is shown in Figure 4.31.

Considering these trends, it can be said that for the stilling basins formed with 40, 50 and 60 cm cubic elements, as the chute channel slope increases the effectiveness in terms of energy dissipation increases. However, for stilling basins formed with 20 and 30 cm cubic elements this effectiveness only increases up to a chute angle of 20 degrees. When the chute angle is further increased to 30 degrees it starts decreasing. In conclusion one can say that for large chute channel angles smaller blocks might be inefficient.

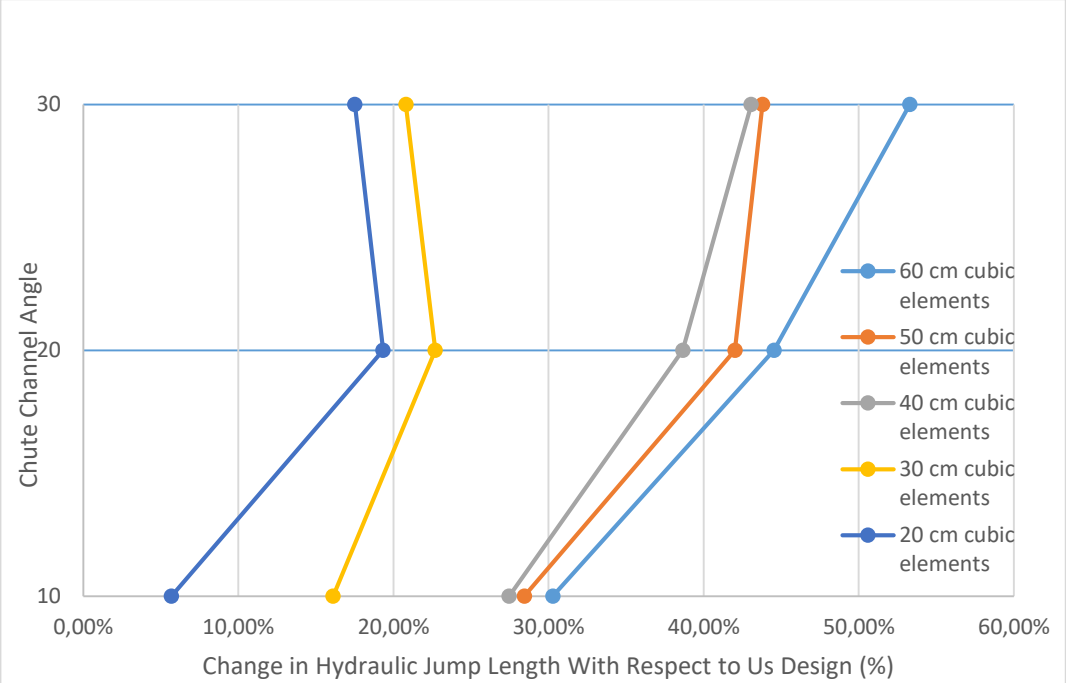

Figure 4.31 Chute Channel Angle-Change in Hydraulic Jump Length with Respect to US Design

Since the start and end points of the hydraulic jump are different for each chute angle and roughness element, knowing the hydraulic jump length or knowing the starting point of the hydraulic jump alone is not enough to show how far the jump is

prolonged over the stilling basin. In Figure 4.32 below, the differences between the lengths and finishing distances of the hydraulic jumps indicated by the oval symbol are presented in scales according to the simulation results. The largest change in the end point of the hydraulic jump is between the 30 cm and 40 cm cubic elements for all the slopes tested.

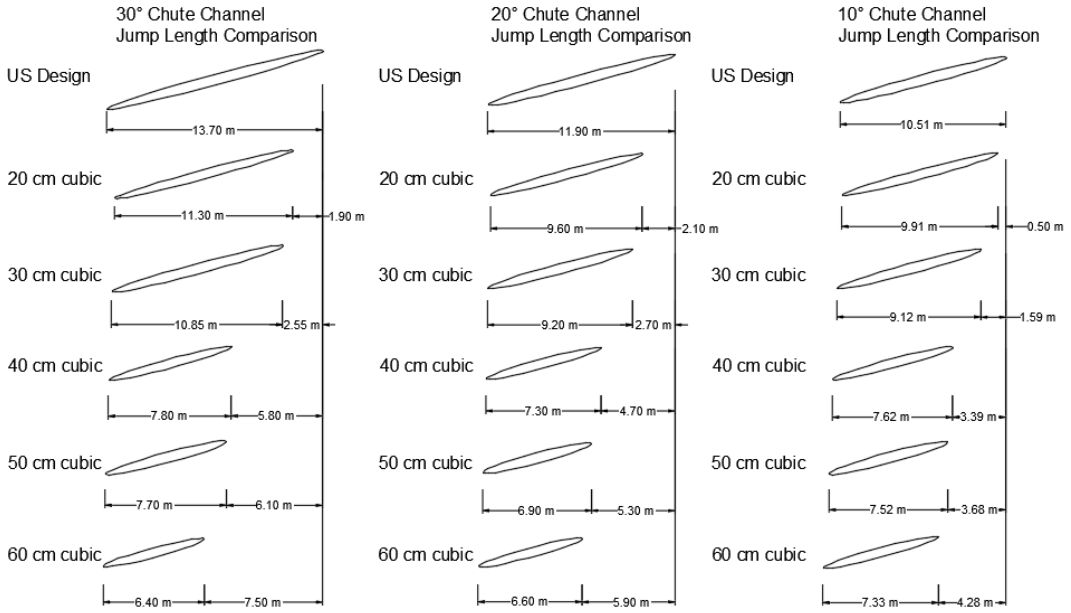

Figure 4.32 The differences between the lengths and finishing distances of the hydraulic jumps for simulated cases.

y_2 and y_1 values obtained from the simulations completed for broad crested weir height of 0.5-meter and chute channel angle 20˚ with 3 meter block-free surface were shared in Table 4.12. According to these results, increase in cubic element size push the jump towards the chute channel like the previous examples. However, there is no direct correlation between the jump length and the block size. Some additional investigation should be made in order to get a more reliable result.

Table 4.12 y_2, y_1,and hydraulic jump length values for 20˚ angle chute channel and 0.5 meter height broad crested weir

	X Coordinate for y_1 (m)	**X Coordinate for y_2(m)**	**Jump Length (m)**
0.2 meter cubic roughness elements with 3 meter blocks-free surface	150.55	162.05	11.50
0.3 meter cubic roughness elements with 3 meter blocks-free surface	148.1	162.85	14.75
0.4 meter cubic roughness elements with 3 meter blocks-free surface	147.65	156.85	9.20

Flow profiles obtained with cubic elements of 0.2 m, 0.3 m and 0.4 m for a weir height of 0.5 m at a chute angle of 20 degrees are shown in Figure 4.33. There are oscillations on the flow surface for 0.3 meter cubic element size. There is also a similar oscillation at the same sized cubic elements over the stilling basin without block-free surface and 0.9-meter broad crested weir height (at a larger flow depth).

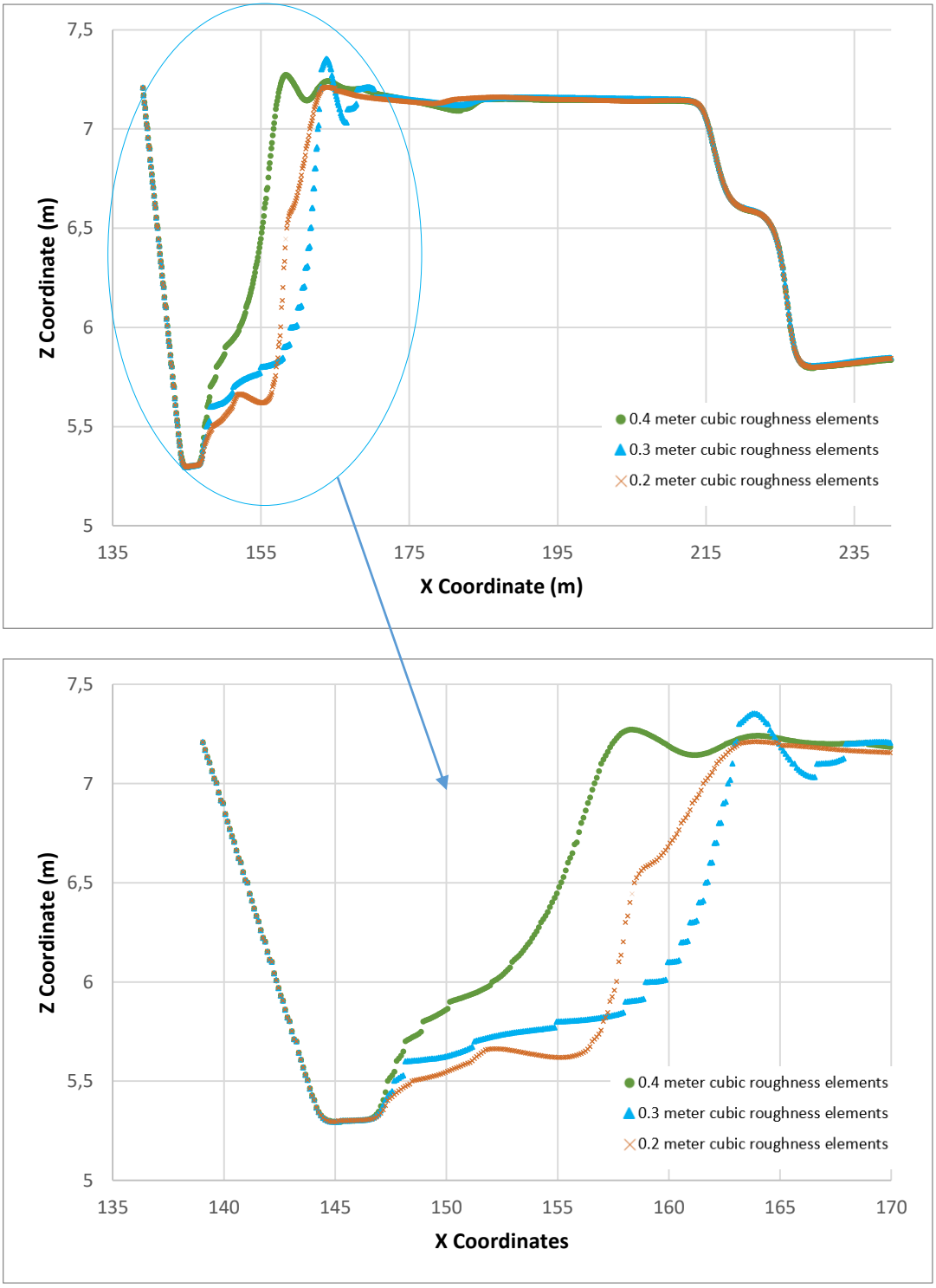

Figure 4.33 Flow profile for 20˚ chute channel and broad crested weir height is 0.5 meter

y_2 and y_1 values obtained from the simulations completed for broad crested weir height of 0.9-meter and chute channel angle 20˚ without block-free surface were shared in Table 4.13. These results show that increase in cubic elements size push the jump towards the chute channel like others. Although the jump length tends to decrease with increasing roughness element size it is not possible to obtain a direct relationship between the jump length and the roughness element size. For this case using 0.6-meter sized cubic elements in the basin causes a sloping apron which means hydraulic jumps occur over the chute channel.

Table 4.13 y_2, y_1, and hydraulic jump length values for 20˚ angle chute channel and 0.9 meter height broad crested weir

	X Coordinate for y_1 (m)	**X Coordinate for y_2(m)**	**Jump Length (m)**
0.2 meter cubic roughness elements	145.05	155.95	10.90
0.3 meter cubic roughness elements	144.25	152.85	8.60
0.4 meter cubic roughness elements	144.15	152.85	8.70
0.6 meter cubic roughness elements	143.25	148.35	5.10

Flow profiles are shown in Figure 4.34 for the broad crested weir height of 0.9-meter and chute channel angle of 20˚. As the size of the cubic elements increase the jump is pushed towards upstream. However, the most drastic shift occurs for the cubic roughness element size of 0.6m.

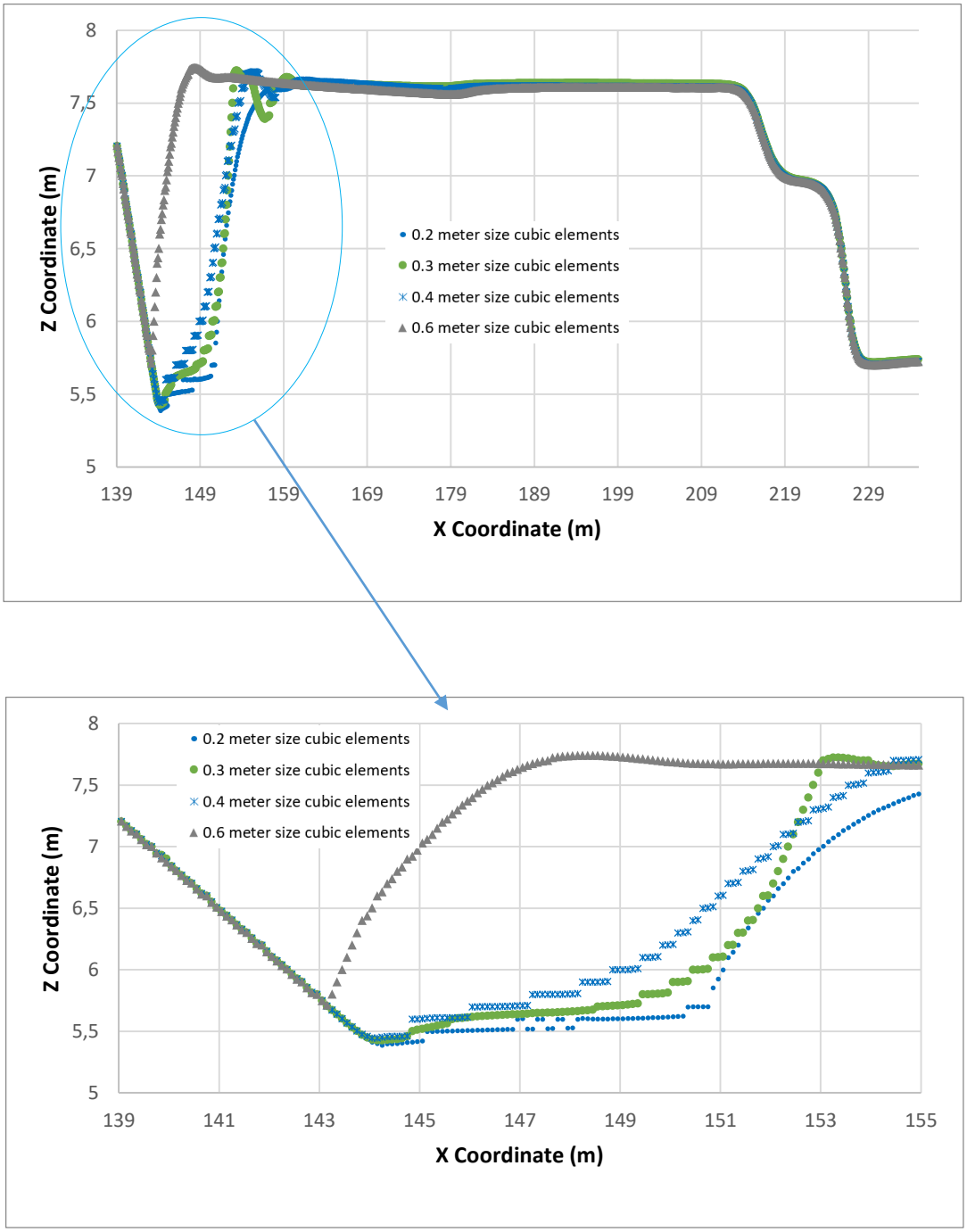

Figure 4.34 Flow profile for 20˚ chute channel and broad crested weir heihgt is 0.5 meter

CHAPTER 5

CONCLUSION

The starting point of this study was how to increase the energy dissipation in a stilling basin compared to US Design type III. Flow 3D model was used to obtained numerical results. For the specified cases, the models were solved for both Type III US Design and stilling basin which is filled with cubic macro roughness elements.

Findings:

1) Hydraulic Jump Length is decreased with cubic roughness elements with respect to US Design. The decrease in hydraulic jump length varied from 5.69% to 53.28% according to used cubic elements and chute channel angle.
2) For all the slopes tested, increase in the dimension of the cubic roughness elements causes a decrease in the hydraulic jump length if the jumps are initiated over the chute channel.
3) The distance from the starting point of the hydraulic jump to the end point of the chute channel (Li) increases in direct proportion to the increase in the dimensions of the cubic elements.
4) As the cubic elements get bigger, the hydraulic jump starts earlier and the hydraulic jump length decreases for the hydraulic jumps which are initiated over the chute channel, so when the cubic elements get bigger the point where the hydraulic jump ends becomes earlier. That's not the same for the US design as in this case the hydraulic jump starts earlier compared to some of the cubic elements (that changes according to chute channel angle) but in any case, the jump ends at a further position.
5) In stilling basins filled with cubic elements, the hydraulic jump ends at an earlier position compared to US Type III design. Therefore, smaller stilling

basins can be designed with cubic elements compared to the US Design Type III.

6) Effectiveness of the cubic elements in terms of energy dissipation increases with chute channel slope for larger blocks (40, 50 and 60 cm blocks), however for smaller blocks (20 and 30 cm blocks) this effectiveness first increases and then starts decreasing with increase in chute channel's slope.
7) When the size of the cubic elements gets closer to the critical flow depth, splashes occurred and formation of the hydraulic jump could not be clearly observed according to the classifiacation specified by Peterka (1958).
8) Macro roughness elements sizes can cause change in the shape of the hydraulic jump under the same flow properties.
9) Lag in the positioning of the roughness blocks in the stilling basin affects the position of the jump in the stilling basin.
10) Locating the roughness elements immediately at the starting point of the stilling basin decreases the hydraulic jump length, however there is a risk for the jump to be initiated over the chute channel.

Recommendations:

1) Different roughness element patterns and shapes can be tested as a future study.
2) Although the average velocity values in the study remained within the limits of Type III, these values were very close to the limit values in the 30-degree chute channel slope. Therefore, increasing the angle at these energy levels exceeds the Type III design criteria.
3) To operate at higher angles, the water level in the reservoir must be lowered.
4) Air entrainment model for Flow-3D can be activated and tested.
5) Dividing the simulation into two parts as chute channel and stilling basin was a very helpful way to decrease the simulation time. It is recommended for the future studies to use this option.

REFERENCES

Bejestan, M. S., & Neisi, K. (2009). A new roughened bed hydraulic jump stilling basin. Asian journal of applied sciences, 2(5), 436-445.

Blaisdell, F. W. (1959). The SAF stilling basin: A structure to dissipate the destructive energy in high-velocity flow from spillways (No. 156). Agricultural Research Service.

Chow, V.T. (1959) Open Channel Hydraulics. McGraw-Hill, New York.

De Padova, D., & Mossa, M. (2021). Hydraulic jump: a brief history and research challenges. Water, 13(13), 1733.

Elevatorski, E. A. (1959). Hydraulic energy dissipators. New York: McGRAW-HILL BOOK COMPANY, INC

Finnemore, E. J., & Franzini, J. B. (2002). Fluid mechanics with engineering, applications. McGraw-Hill Education.

Frizell, K. W., & Svoboda, C. D. (2012). Performance of type III stilling basins–stepped spillway studies. Hydraulic Laboratory Report HL-2012-02, US Bureau of Reclamation, Denver, USA.

Hager, W. H., & Bremen, R. (1989). Classical hydraulic jump: sequent depths. Journal of hydraulic research, 27(5), 565-585.

Hughes, W.C., and Flack, J.E.(1984) "Hydraulic Jump Properties Over a a Rough Bed", J. of Hydraulic Engineering, 110(12),1755-1771.

Husain, D., Alhamid, A. A., & Negm, A. A. M. (1994). Length and depth of hydraulic jump in sloping channels. Journal of Hydraulic Research, 32(6), 899-910.

Leutheusser, H. J., & EJ, Schiller (1975). Hydraulic Jump in a Rough Channel.

Manning's roughness coefficients. https://www.engineeringtoolbox.com/mannings-roughness-d_799.html.

Mohamed Ali, H. S. (1991). Effect of roughened-bed stilling basin on length of rectangular hydraulic jump. Journal of Hydraulic Engineering, 117(1), 83-93.

Negm, A. M. (2002, September). Optimal roughened length of prismatic stilling basins. In Proceedings of the 5th International Conference on Hydro-Science and Engineering, Poland.

Peterka, A. J. (1958). Hydraulic design of spillways and energy dissipators. A water resources technical publication, engineering monograph, 25.

Pourabdollah, N., Heidarpour, M., Abedi Koupai, J., & Mohamadzadeh-Habili, J. (2022). Hydraulic jump control using stilling basin with adverse slope and positive step. ISH Journal of Hydraulic Engineering, 28(1), 10-17.

Rajaratnam, N., & Muralidhar, D. (1968). Characteristics of the rectangular free overfall. Journal of Hydraulic Research, 6(3), 233-258.

Tokyay, N. D. (2005). Effect of channel bed corrugations on hydraulic jumps. In Impacts of Global Climate Change (pp. 1-9).

Tran, C. K., Vo, H. C., La, H. P., Le, B. T. H., Dang, N. D., Le, T. N., ... & Hoang, T. D. (2022). An Experimental Study of Roughness Elements to Design Fixed-Bed Hydraulic Model—A Step-by-Step Process and an Application in Vietnam. Water, 15(1), 72.

U.S. Bureau of Reclamation (USBR). (1987). Design of Small Dams, U.S. Government Printing Office, Washington, D.C.

USBR (United States Bureau of Reclamation Webpage). https://www.usbr.gov/.

Velioglu, D. E. N. I. Z., Tokyay, N. D., & Dincer, A. I. (2015, June). A numerical and experimental study on the characteristics of hydraulic jumps on rough beds. In E-proceedings of the 36th IAHR World Congress (Vol. 28, pp. 1-9).